RSC Advances

This is an *Accepted Manuscript*, which has been through the Royal Society of Chemistry peer review process and has been accepted for publication.

Accepted Manuscripts are published online shortly after acceptance, before technical editing, formatting and proof reading. Using this free service, authors can make their results available to the community, in citable form, before we publish the edited article. This *Accepted Manuscript* will be replaced by the edited, formatted and paginated article as soon as this is available.

You can find more information about *Accepted Manuscripts* in the Information for Authors.

Please note that technical editing may introduce minor changes to the text and/or graphics, which may alter content. The journal's standard Terms & Conditions and the Ethical guidelines still apply. In no event shall the Royal Society of Chemistry be held responsible for any errors or omissions in this *Accepted Manuscript* or any consequences arising from the use of any information it contains.

ROYAL SOCIETY OF CHEMISTRY

www.rsc.org/advances

New aryloxy-quinone derivatives as potential Anti-Chagasic agents: Synthesis, trypanosomicidal activity, electrochemical properties, pharmacophore elucidation and 3D-QSAR analysis

Karina Vázquez, Christian Espinosa-Bustos, Jorge Soto-Delgado, Ricardo A. Tapia, Javier Varela, Estefanía Birriel, Rodrigo Segura, Jaime Pizarro, Hugo Cerecetto, Mercedes González, Margot Paulino and Cristian O. Salas

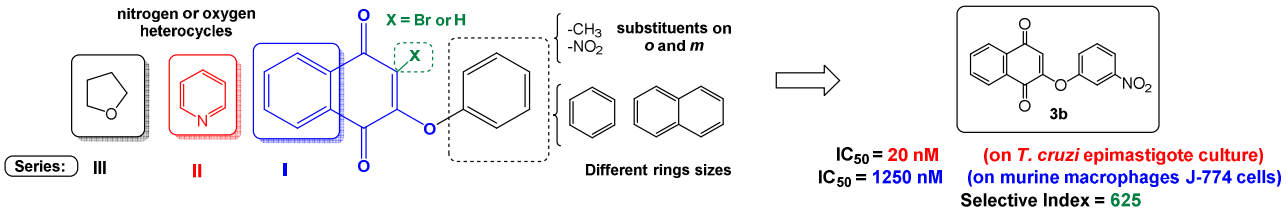

RSC Advances Accepted Manuscript

New aryloxy-quinone derivatives as potential Anti-Chagasic agents: Synthesis, trypanosomicidal activity, electrochemical properties, pharmacophore elucidation and 3D-QSAR analysis

Karina Vázquez [a], Christian Espinosa-Bustos [a], Jorge Soto-Delgado [b], Ricardo A. Tapia [a], Javier Varela [c], Estefanía Birriel [c], Rodrigo Segura [d], Jaime Pizarro [d], Hugo Cerecetto [c,e], Mercedes González [c], Margot Paulino [f],* and Cristian O. Salas [a],*

[a] *Departamento de Química Orgánica, Facultad de Química, Pontificia Universidad Católica de Chile, Santiago 6094411, Chile.*

[b] *Departamento de Ciencias Químicas, Facultad de Ciencias Exactas, Universidad Andrés Bello, Quillota 980, Viña del Mar, Chile.*

[c] *Grupo de Química Medicinal, Instituto de Química Biológica, Facultad de Ciencias, Universidad de la República, Iguá 4225, Montevideo, Uruguay.*

[d] *Departamento de Química de los Materiales, Facultad de Química y Biología, Universidad de Santiago de Chile, Santiago 9170022 Chile.*

[e] *Área de Radiofarmacia, Centro de Investigaciones Nucleares, Facultad de Ciencias, Universidad de la República, Mataojo 2055, Montevideo, Uruguay.*

[f] *Centro de Bioinformática Estructural-DETEMA, Facultad de Química, Universidad de la República, C.C. 1157, Montevideo, Uruguay.*

*Corresponding authors. e-mail address: margot@fq.edu.uy (M. Paulino) and cosalas@uc.cl (C.O. Salas).

Abstract

A set of new aryloxy-quinones were synthesized and evaluated *in vitro* against the epimastigote form of *Trypanosoma cruzi* and their unspecific cytotoxicity was tested on murine macrophages J-774 cells. Most of these novel compounds were found to be extremely more potent and selective than the standard drug nifurtimox. Interestingly, 2-phenoxy-naphthoquinone **3b** displayed a remarkable nanomolar inhibitory activity, IC_{50} = 20 nM, and a high selectivity index, SI = 625. The E_{pc1} was determined for the most interesting compounds and no correlation with the trypanosomicidal effect was found. Therefore, an *in silico* study was carried out to obtain a pharmacophoric model and quantitative structure-trypanosomicidal activity relationship. The designed pharmacophore recognized the more potent and selective molecules, exhibiting five pharmacophoric features. A correlation coefficient R^2 of 0.99 of pIC_{50} plotted against the predicted values indicated that the 3D-QSAR equation could be applied to further predictions of newly designed trypanosomicidal compounds.

RSC Advances Accepted Manuscript

1 Introduction

Chagas disease, caused by the protozoan parasite *Trypanosoma cruzi* (*T. cruzi*), is a neglected tropical endemic disease in Central and South America.[1] As a result of international migrations, Chagas disease is also found now in non-endemic countries such as in the United States,[2] Europe[3] and Australia.[4] In these countries where the vectors do not exist, the infection can be transmitted through donation of infected blood or organs, and through vertical transmission from mother to child.[5] The World Health Organization (WHO) estimates that about 10 million people worldwide are currently infected, mainly in endemic areas of Latin America. This disease represents an important health problem in Central and South America and although mortality indexes have been decreased in the last few years, actually more than 10.000 deaths are estimated to occur annually from Chagas disease.[6] This disease has two successive clinical phases: acute and chronic. There are two main drugs used for the treatment, benznidazole and nifurtimox, developed more than 40 years ago, exhibit limited efficacy in the chronic phase and both present severe toxic side effects.[7, 8] The need of more effective drugs has stimulated the search for new compounds with potential clinical utility.

In view of the structural diversity and wide range of pharmacological activities exhibited by compounds having a quinone scaffold, many natural and synthetic naphthoquinones have been tested against *T. cruzi* parasites as possible anti-Chagas agents.[9, 10] Thus, considering the important anti-trypanosomal and leishmanicidal activity exhibited by lapachol (**I**, Fig. 1), Bolognesi and co-workers have synthesized a small library of 2-aryloxy-1,4-naphthoquinone derivatives.[11] The most active compound was 2-phenoxy-1,4-naphtoquinone **II** (Fig. 1), which showed an IC_{50} of 1.70 μM against the amastigote forms of *T. cruzi*, but with low selectivity index (SI < 5).[11]

In the search for new compounds with improved trypanosomicidal activity, we have been focused in the synthesis of new aryloxy-indolequinones with different substitution patterns, which were tested for their trypanosomicidal effect and selectivity in cultures of *T. cruzi* epimastigotes and macrophages, respectively. Interestingly, 6-phenoxyindolequinone **III** (Fig. 1), displayed excellent nanomolar inhibitory activity, IC_{50} = 20 nM, and high selectivity index, SI = 625.[12] Based on these results, we recently carried out a study of 2-arylaminonaphthoquinone and 5*H*-benzo[*b*]carbazole-6,11-dione derivatives. These compounds were assayed against *T. cruzi* epi- and trypomastigotes and some of them against cancer cells and normal fibroblasts.[13] It was found that certain chemical modifications on the naphthoquinone moiety increase the trypanosomicidal and cytotoxic effects. Several of these compounds were more potent than the reference drug nifurtimox against both stages of the parasite and

RSC Advances Accepted Manuscript

exhibited increased selectivity against *T. cruzi* in comparison with VERO cells, being the most active 2-arylaminonaphthoquinone **IV** (Fig. 1). On the other hand, the 2-phenyl-aminonaphthoquinone **V** showed significant *in vitro* cytotoxicity against prostate and mammary cancer cells and high selectivity in respect to fibroblasts. A preliminary analysis confirmed an earlier conclusion that the replacement of a benzene ring by a pyridine ring condensed to the quinone core is an important modification to increase these activities.[14, 15] The attempts to disclose a general structure-activity relationships using stereoelectronic and lipophilicity properties, point out that the presence of a chlorine atom at C-3 and a highly lipophilic alkyl group or aromatic ring are newly observed elements with the aim of to design more selective cytotoxic and trypanosomicidal compounds.[13]

On the other hand, quantitative structure-activity relationship (QSAR) studies have emerged as a useful tool to find relevant physicochemical descriptors for the design of new drugs,[16, 17] as well as to get some insight into the underlying mechanisms of action of the QSAR-based predicted activities. Recently, QSAR analysis was applied to naphthoquinone derivatives and can be useful in the search for new compounds with enhanced anti-trypanosomal activity.[18-20]

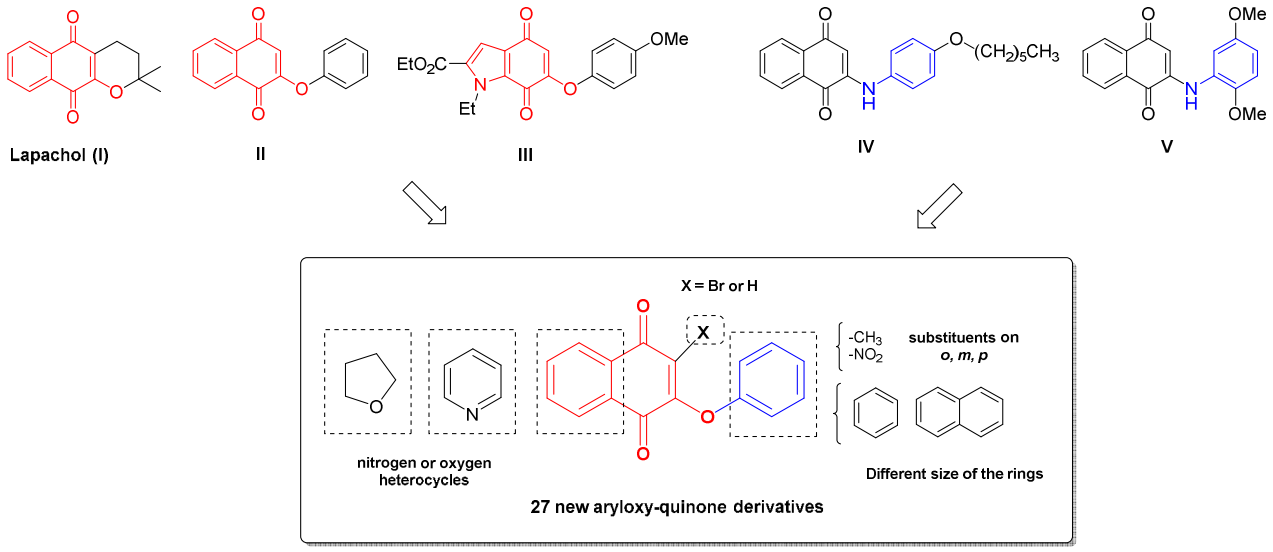

Fig. 1 Chemical structures of lapachol, phenoxy- and phenylamino-quinones with trypanosomicidal activities and designed template for new anti-*T. cruzi* agents.

Herein, we designed a set of 27 new molecules based on the aryloxy- quinone scaffold (Fig. 1), which combine two pharmacophoric patterns of trypanosomicidal compounds (**II-V**). These new compounds could validate our hypothesis that chemical modifications on the naphthoquinone core or aromatic ring would increase the trypanosomicidal effects and the selectivity as well. The *in vitro* trypanosomicidal

RSC Advances Accepted Manuscript

activity against *T. cruzi* epimastigotes and the selectivity index for the set of 27 compounds was evaluated. Additionally, considering that a possible mechanism of action is by reduction of the quinone system and production of free-radical intermediates,[15, 21] the electrochemical properties for most active compounds were evaluated in order to find a probable correlation with their anti-*T. cruzi* activity. Furthermore, an *in silico* strategy was applied to obtain a pharmacophoric model and 3D-QSAR equation, to analyze the *in vitro* trypanosomicidal activity of the compounds under study.

2 Results and discussion

2.1 Chemistry

A useful and direct approach for the synthesis of required aryloxy-quinones is through nucleophilic substitution reaction of phenols with haloquinones in basic medium at room temperature.[11, 22] As shown in Scheme 1, 2-aryloxy-naphthoquinones **3a-f** (series **I**) were obtained in 40-97% through reaction of phenols **2a-c** with halonaphthoquinone **1a** or **1b** in dimethylformamide (DMF) in the presence of potassium carbonate. Similarly, reaction of halonaphthoquinone **1a** or **1b** with naphthols **2d**,**e** afforded the corresponding naphthoquinones **3g-j** in 53-95% yield.

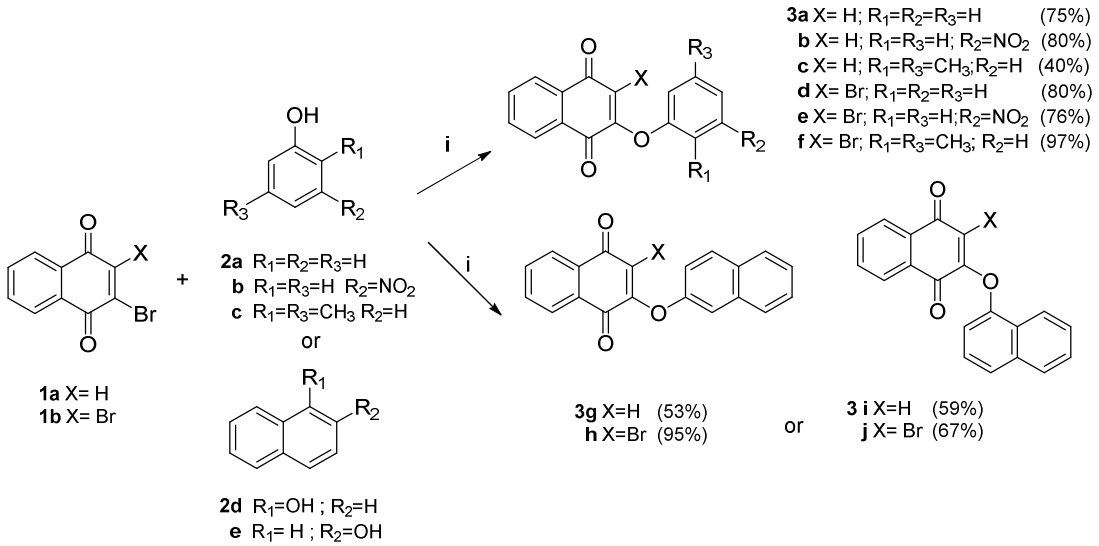

Scheme 1. Synthesis of compounds of series **I** (**3a-j**). Reagents and conditions: (i) K_2CO_3, DMF, rt, 2-3 h.

The compounds belonging to series **II** were synthesized starting from bromoquinolin-5,8-diones **6a** and **6b** (Scheme 2). These quinones were obtained by bromination (Br_2/MeOH) of 8-hydroxyquinoline **4a** or 8-hydroxy-2-methylquinoline **4b** and subsequent oxidation of the corresponding dibromophenols

RSC Advances Accepted Manuscript

5a,b with nitric acid.[23] The reaction of **6a** and **6b** with the phenols **2a-c** or naphthols **2d,e** furnished regiospecifically the corresponding 7-aryloxy-quinoline-5,8-dione derivatives **7a-i** (24-92% yield).

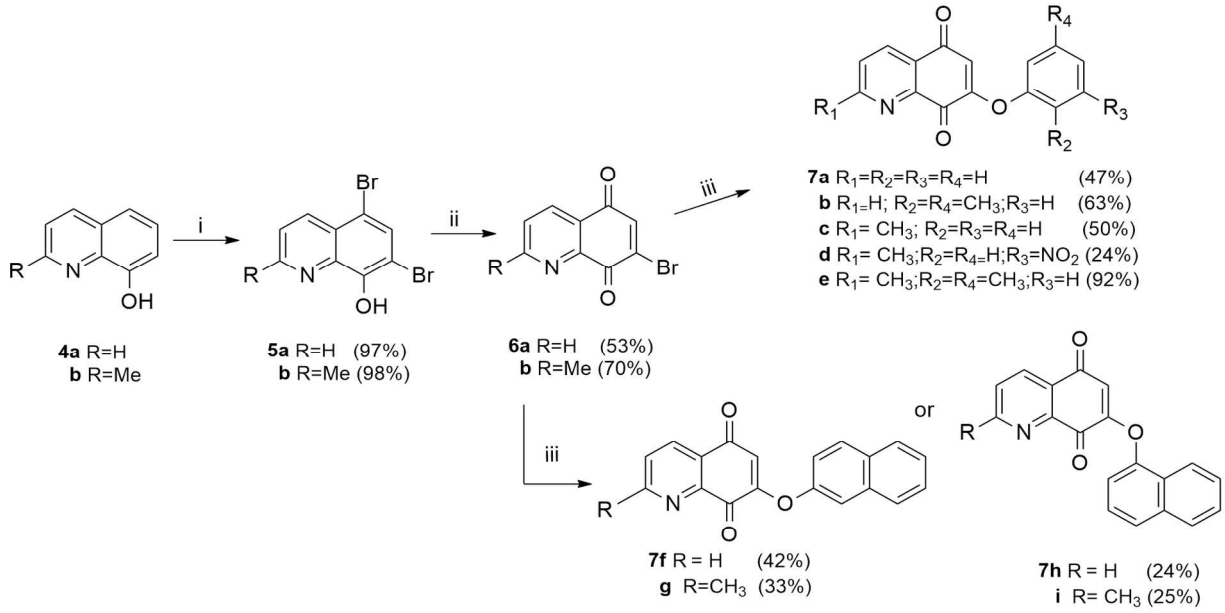

Scheme 2. Synthesis of compounds of series **II** (**7a-i**). Reagents and conditions: (i) Br_2, MeOH, rt, 5 min; (ii) HNO_3, H_2SO_4, 0 °C, 30 min;[23] (iii) K_2CO_3, **2a-e**, DMF, rt, 3-5 h.

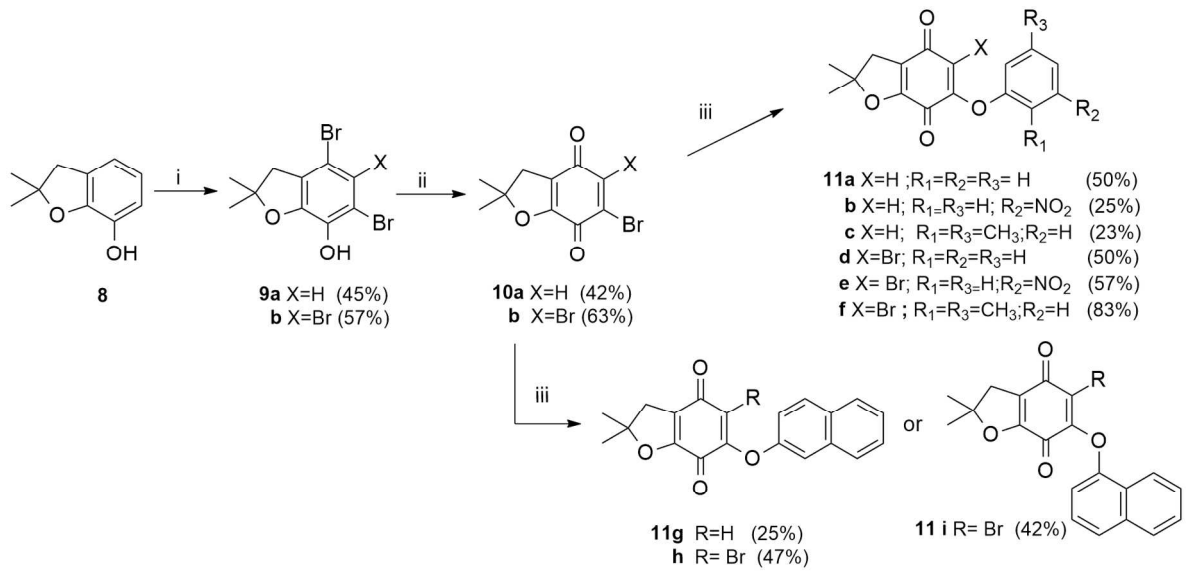

Scheme 3. Synthesis of compounds of series **III** (**11a-i**). *Reagents and conditions:* (i) Br_2, $CHCl_3$, rt, 1.5 h; (ii) CrO_3, H_2O/AcOH, rt, 2 h; (iii) K_2CO_3, DMF, **2a-e**, rt, 2 h.

RSC Advances Accepted Manuscript

The required bromobenzofuran-4,7-diones **10a,b** (Scheme 3), were obtained using phenol **8** as substrate. The bromination of **8** with two or four equivalents of Br_2 in $CHCl_3$, followed by oxidation with chromium trioxide, yielded the halobenzofuranquinones **10 a,b**.[14] The reaction of **10a,b** and the phenols **2a-e** afforded compounds **11a-i** (series **III**) in 23-83% yield. The chemical structures of the target compounds were established on the basis of their spectral properties (IR, ^{1}H NMR, ^{13}C NMR and HRMS, see experimental part and supplementary material).

2.2 Trypanosomicidal effect

The *in vitro* trypanosomicidal activity of 2-aryloxy-naphthoquinones **3a-j** (series **I**), 7-aryloxy-quinolinquinones **7a-i** (series **II**) and 6-aryloxy-furonaphthoquinones **11a-i** (series **III**), was initially tested against the epimastigote form of *T. cruzi*, Y strain (Tc II).[24] For each derivative a dose-response assay, between 0.01 and 50 μM, was assayed to calculate the IC_{50} concentration (50% inhibitory concentration). Nifurtimox (Bayer) was used as the reference trypanosomicidal drug.[25, 26] All aryloxy-quinones exhibited a potent trypanosomicidal activity and they were more active than the reference drug nifurtimox, which had an IC_{50} of 7.0 μM (Table 1). Among them, compounds **3a-b**, **7f** and **7h** displayed the most potent inhibitory activity with values of IC_{50} in the nanomolar order (IC_{50} < 90 nM for epimastigotes).

2-Phenoxy-1,4-naphthoquinone **3a** (IC_{50} = 50 nM), was selected as a reference compound to evaluate the effect of the chemical modifications for compounds of the series **I**. It was found that the incorporation of a withdrawing group in the aryloxy moiety (nitro derivative **3b)**, enhanced the trypanosomicidal effect and the compound with highest activity (IC_{50} = 20 nM) was obtained. On the other hand, the electron donating methyl groups (**3c**) or α- and β-naphthyl rings (**3g,i**), weakly decreased the trypanosomicidal effect compared to **3a**, but these compounds were still more active than nifurtimox (40 times). Regarding the replacement of the hydrogen atom at C-3 by bromine, compounds **3d-f** showed a decrease in trypanosomicidal effect compared with their un-halogenated analogs; whereas 2-naphthyloxyquinones **3h,j** kept their anti-trypanosoma activity. A similar behavior was observed for the 2-phenylamino-1,4-naphthoquinone derivatives previously studied.[13]

For the compounds belonging to the series **II** (**7a-i**), the most active were **7f** and **7h** (IC_{50} = 40 and 90 nM respectively). In this case, the presence of the α- or β-naphthyl ring bound to the quinone core, increased the trypanosomicidal effect in comparison to the reference compound **7a** (IC_{50} = 110 nM), in contrast to the results for the series **I**. The nitro derivative **7d** was the less active of this series, but still

RSC Advances Accepted Manuscript

it was more potent than nifurtimox (16 fold). The presence of methyl substituents on the phenyl ring of **7a** had no effect on the activity (**7b**). However, the trypanosomicidal activity of quinoline derivatives with a methyl group at C-2 was lower than their H-analogues, showing a decrease up to four times (**7f** *vs* **7g**). Finally, analyzing the replacement of the benzene by a pyridine ring (series **I** *vs* **II**), an increase in trypanosomicidal effect was observed on the epimastigote form (except **3a** vs **7a**). For instance, compound **7f** is almost four times more potent than its carbocyclic analog **3g**, with IC_{50} values of 40 nM and 150 nM, respectively. These results are in agreement with previous findings from our group that indicate the relevance of nitrogen substitution in the aromatic ring for activity of related compounds.[13-15]

The dihydrofurane derivatives of the series **III** (**11a-i**), were less active than the other series being most of the IC_{50} values > 1.0 μM, except compound **11c** which showed the lowest IC_{50} value (0.54 μM). These results suggest that oxygen heterocyclic system fused to the quinone ring, decrease the trypanosomicidal effect and that the halogen replacement at the quinone ring, give compounds with less activity.

A preliminary analysis of several modifications on the naphthoquinone core showed a significant improvement in the trypanosomicidal activity in compounds bearing nitro group substitution (**3b**) and the replacement of a benzene ring by pyridine ring (**7f** and **7h**), in comparison to the reference compound **3a**.

2.3 Selectivity Studies

Compounds with trypanosomicidal activity do not have pharmacological relevance when display high cytotoxicity on mammalian host cells and therefore exhibits low selectivity. For this reason, compounds with the highest trypanosomicidal effect were studied for their unspecific cytotoxicity on murine macrophages J-774 cells and the selective indexes (SI) were calculated as the ratio of the IC_{50} between epimastigotes and J-774 cells (Table 1). According to some authors in the search of new strategies for the development of novel drugs for tropical disease, the selective index should be higher than 50.[27, 28] Table 1 shows the IC_{50} values for the most compounds on J-774 cells and these results concluded that most of them (19 compounds) exhibited a better selectivity than nifurtimox (SI value = 40). Interestingly, compounds **3a**, **3b**, **3d**, **3e**, **3f**, **3j**, **7a**, **7b**, **7f**, **7g** and **7h** included in series **I** and **II** showed a high selectivity index (SI values > 100). Among them, compound **3b** deserved a special importance, because exhibited the highest trypanosomicidal activity (IC_{50} value of 20 nM) and an

RSC Advances Accepted Manuscript

elevated selectivity in regard to its toxicity toward J-774 cells (SI value = 625). A second group of compounds (**3c**, **3g**, **3h**, **3i**, **7c**, **7e**, **7i** and **11c**) were slightly more selective than nifurtimox (SI values among 70-90). Finally, a third group of compounds (**11a**, **11b**, **11d**, **11g**, **11h**, **11i** and **7d**) were less selective than nifurtimox (SI < 20) and most of them belonged to compounds of the series **III**, which showed the lowest trypanosomicidal activity.

A preliminary chemical structural analysis for the selectivity indicates that for those compounds of the series **I**, the presence of the nitro group in the aryloxy moiety (**3b** and **3e**) contributed to an increase of both the trypanosomicidal effect and selectivity. The opposite effect was observed in the presence of dimethylphenyl (**3c**) or naphthyl groups (**3g** and **3i**), that increased the toxicity in mammals and decreased selectivity.

In previous studies, our group had reported that the substitution of hydrogen by halogen at C-2 in the quinone moiety increase the selectivity,[13] nevertheless, for halogenated compounds (**3d-f**, **3h** or **3j**), there is no a clear pattern. On the other hand, for those of the series **II** (regarding to **7a**, SI = 200), the presence of the β-naphthyl group linked to the naphthoquinone provides an access to more selective compounds (**7f**). In contrast, the replacement of the quinoline core by 2-methylquinoline in addition to the aryloxy substitution by dimethylphenyl or α-naphthyl ring, reduced significantly the selectivity in all analogues.

There are several proposed mechanisms of action for the trypanosomicidal activity of quinone derivatives that could be related with the selectivity shown in this study. One of them is the well-known ability of quinones for generating reactive oxygen species (ROS) through redox cycle with molecular oxygen and consequently strong oxidative stress and cell death.[10, 29-32] The biochemical difference between the parasite and host cells to avoid the damage mediated by ROS, are considerable, meanwhile mammalian cells defend themselves efficiently against free radicals in diverse ways,[33] *T. cruzi´*s defense mechanisms against oxidative stress are defective.[34] On the other hand, it has been reported that quinones are inhibitors of trypanothione reductase (TR), an enzyme that constitute part of the principal oxidative-stress defense of the *T. cruzi* [35, 36] and it is absent in the mammals. Studies on this issue are currently developed in our laboratory.

RSC Advances Accepted Manuscript

Table 1. Effect upon culture growth of *T. cruzi* and selectivity index *vs* J-774 cells, and the E_{pc1} of aryloxy-quinones.

Entry	IC_{50} (μM)[a]	J-774 IC_{50} (μM)	S.I.[b]	E_{pc1} (V)[c]
3a	0.05 ± 0.02	<12.5	<250	-0.610
3b	0.02 ± 0.01	12.5	625	-0.526
3c	0.17 ± 0.05	<12.5	<73.5	-0.610
3d	0.11 ± 0.04	18	163.6	-0.397
3e	0.11 ± 0.04	46	418.2	-0.369
3f	0.23 ± 0.06	39	169.6	-0.397
3g	0.15 ± 0.04	<12.5	<83.3	-0.633
3h	0.14 ± 0.05	<12.5	<89.3	-0.456
3i	0.17 ± 0.04	<12.5	<73.5	-0.624
3j	0.17 ± 0.06	19	111.8	-0.440
7a	0.11 ± 0.04	22	200	-0.517
7b	0.11 ± 0.04	18	163.6	-0.555
7c	0.14 ± 0.05	12.5	89.3	-0.566
7d	0.44 ± 0.09	12.5	28.4	-0.515
7e	0.23 ± 0.07	<12.5	<54.3	-0.608
7f	0.04 ± 0.02	15	375	-0.508
7g	0.15 ± 0.04	16	106.7	-0.536
7h	0.09 ± 0.04	<12.5	<138.9	-0.517

RSC Advances Accepted Manuscript

Entry	IC_{50} (μM)[a]	J-774 IC_{50} (μM)	S.I.[b]	E_{pc1} (V)[c]
7i	0.17 ± 0.05	<12.5	<73.5	-0.527
11a	1.00 ± 0.02	21	21	-0.550
11b	2.30 ± 0.03	61	25.5	-0.456
11c	0.54 ± 0.13	44	81.5	n.d.[d]
11d	5.00 ± 0.6	25	5.00	-0,347
11e	1.60 ± 0.2	n.d.	n.d.	n.d.
11f	1.80 ± 0.4	n.d.	n.d.	n.d.
11g	0.98 ± 0.17	21	21.4	-0.508
11h	7.00 ± 1.7	~ 25	~ 3.60	-0.482
11i	5.50 ± 0.4	~ 25	~ 4.54	-0.465
Nfx[e]	7.00 ± 0.3	316 ± 0.5	40	-

[a] The results are mean of three independent experiments.

[b] Selectivity Index: expressed as the ratio of IC_{50} in J-774 cells to IC_{50} in epimastigotes.

[c] Values determinate at c = 1 x 10-3 mol L-1, in DMF/TBAP, 0.1 mol L-1, ν = 50 mV s^{-1}.

[d] n.d.: not determined.

[e] 5 μM was used for this assay.

2.4 Pharmacophore elucidation

In order to generate a pharmacophore model (hypothesis), the compound with the highest trypanosomicidal activity (**3b**, IC_{50} 20 nM) was chosen as a structural template. Once the tridimensional structure of the selected molecule **3b** was created, the pharmacophore hypothesis was generated using the polar-charged-hydrophobic (PHC) scheme of MOE program.[37] Several structural particularities were identified: a quinonic ring, aromatic rings, nitro group, and an oxygen bridge with

RSC Advances Accepted Manuscript

the aromatic ring. Thus, using **3b** as template and with the PCH scheme, that combines polarity, charge and hydrophobicity, different pharmacophoric features centered in the middle of the atomic sets (centroids), with aromaticity (Aro), rings with π delocalization (Pir), positive charge (Cat), negative charge (Ani), and hydrogen acceptor capacity (Acc) were defined (Fig. 2).

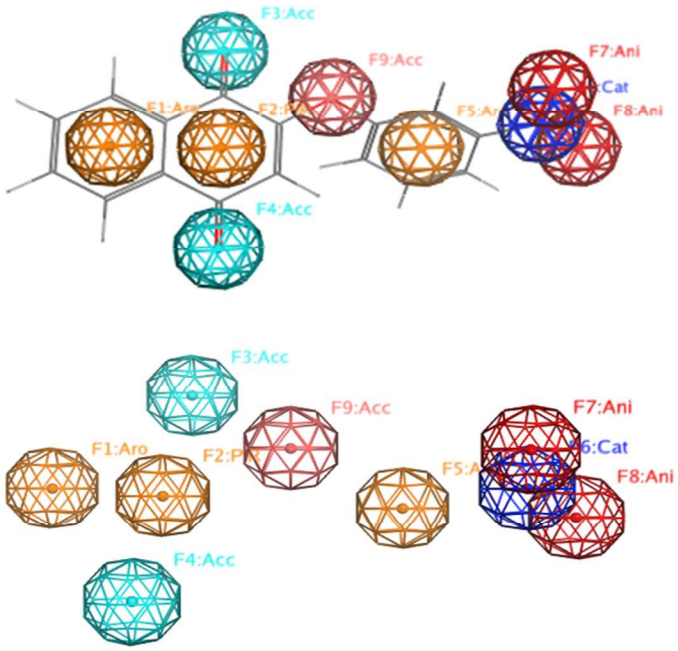

Fig. 2 a) Pharmacophore generated from **3b** overlapped with a rod drawing of molecules; **b)** Pharmacophoric features depicted in the pharmacophore of **3b**. **F1; F5** = Aro, Aromatic moiety; **F2** = Pir, Rings with pi delocalization; **F3; F4; F9** = Acc, hydrogen bond acceptor; **F6** = Cat, cationic; **F7; F** = Ani, anionic.

Once the five pharmacophoric features of **3b** were identified, a combination of them, selecting as essential Aromatic (Aro) and hydrogen acceptor (Acc) (Fig. 3) and taking any four of them each time, the search algorithm reached to found just the molecules with selectivity index greater than 100. By this way, a search was made over the quinone databases and all the eleven selective molecules were found as hits: **3b, 3e, 7f, 7a, 3f, 7b, 3d, 3j, 3h, 7c** and **7d**. From them, all the selective molecules except one (**7g**), were detected, having an 89% of recovering of true positives. Three molecules (**3h**, **7c** and **7d**) are false positives that are; they are non-selective being detected by the pharmacophore as positives. To have a quantitative measurement of this result, it is useful to calculate the enrichment factor R (Equation 1).

RSC Advances Accepted Manuscript

R = [number of selective hits (=8) / number of non-selective hits (=17)] / [number of all selective (=9) / number of all non-selective (=19)] = **0.99** (1)

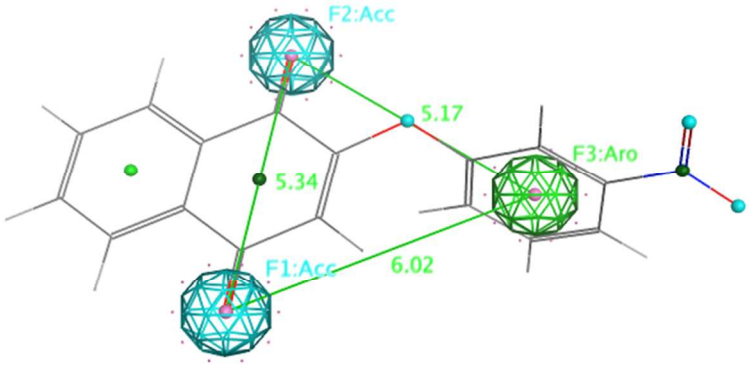

Fig. 3 Selective pharmacophore features and interatomic distances between the essential features Acc (F1 and F2) and Aro (F3).

2.5 Electrochemical study

The cytotoxicity of quinones has been mainly attributed to two processes; redox cycling that generates ROS or electrophilic arylation of critical cellular nucleophiles, in both cases the single-electro-reduction of the quinone ring is the first step. Accordingly, several attempts to establish some correlation between the biological activity and redox potentials of quinones have been reported.[38-41] Cyclic voltammetry (CV) is commonly used to obtain electrochemical parameters for biological studies with quinones, such as potentials of the oxidation (E_{pa}) and reduction (E_{pc}) peaks or E_{redox} (for reversible systems).[38-43] Therefore, redox properties for the most active compounds of each series were determinate by CV in a typical measurement.

Fig. 4 shows the cyclic voltammograms for the most active compounds of each series (for the rest compounds, CV profiles are available in the supplementary information). All quinones exhibited quasi-reversible reduction behavior, which is a typical quinone/semiquinone/hydroquinone triad in equilibrium, and the overall CV profiles are similar to those reported for other quinones.[38, 39, 44, 45]

The E_{pc1} values were obtained from the CV profile of each compound (Table 1), which is most commonly used to compare biological activities. For compounds from the series **I**, the relative reduction potential is as follows: **3e** > **3d** ~ **3f** > **3j** > **3h** > **3b** > **3a** ~ **3c** > **3i** > **3g**. An interesting characteristic that present the five compounds that are most easily reduced, is the presence of the

RSC Advances Accepted Manuscript

bromine direct attachment of the quinone core, which is according to the electron-withdrawing feature of this halogen. The reduction trend for compounds of the series **II** was **7f** > **7d** > **7a** ~ **7h** > **7i** > **7g** > **7b** > **7c** > **7e**. The values for the E_{pc1} for these compounds were around -0.50 V, value which is smaller than those having a halogen of the series **I** and confirm the effect of this substituent. However, the replacement of the benzene ring by the pyridine ring facilitates the electron transfer due to the nitrogen atom attached to the quinone moiety. On the other hand, the presence of an electron-donating methyl group (in either aromatic rings), increased the barrier to reduction (**7i**, **7g**, **7b**, **7c** and **7e**) except for **7d**, which could be related to the presence of nitro group in *meta*-position of the phenyl moiety. The ease of reduction in the series **III**, expressed by E_{pc1} (Table 1) was: **11d** > **11b** > **11i** > **11h** > **11g** > **11a**. All of them display behavior similar to that observed for other benzofuranquinones. The first four compounds of this series shares the presence of a bromine or nitro group as substituent, which confirm the role of these substituents in the reduction process, diminishing the values of the E_{pc1}.

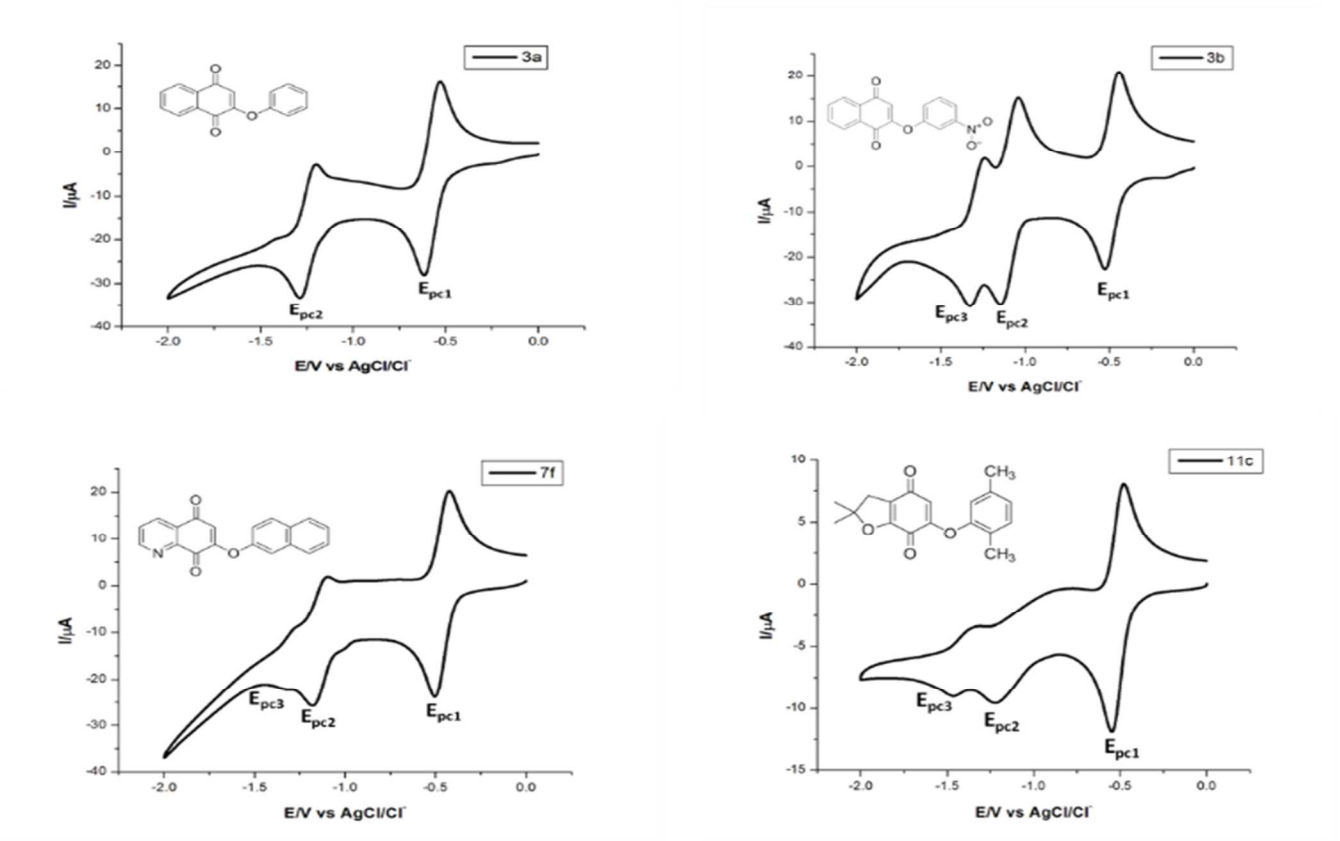

Fig. 4 Cyclic voltammograms of quinones **3a**, **3b**, **7f** and **11c** (1.0 mM). DMF/TBAP (0.1 M), glassy carbon electrode, cathodic direction, scan rate 50 mV s^{-1}.

RSC Advances Accepted Manuscript

However, attempts to reveal an eventual structure-activity relationship using values of Epc1 and pIC_{50} were unsuccessful for each series (Fig. 5). The lack of correlation between these parameters could indicate that the first reduction potential of these aryloxy-quinones is not decisive in the trypanosomicidal activity or although essential for cellular event, not always show a quantitative correlation with this property.[39] In fact, many other factors such as lipophilicity, membrane permeability, etc., need critical consideration in order to rationalize the relationship of structural pattern and trypanosomicidal activity. Considering the small correlation between de Epcl and the pIC_{50}, the search for other tools to understand the trypanosomicidal activity were explored. With this goal in mind, we performed the generation of 3D-QSAR models to correlate chemical structures of quinones with their biological data to identify specific features that influence the observed trypanosomicidal properties.[46-49]

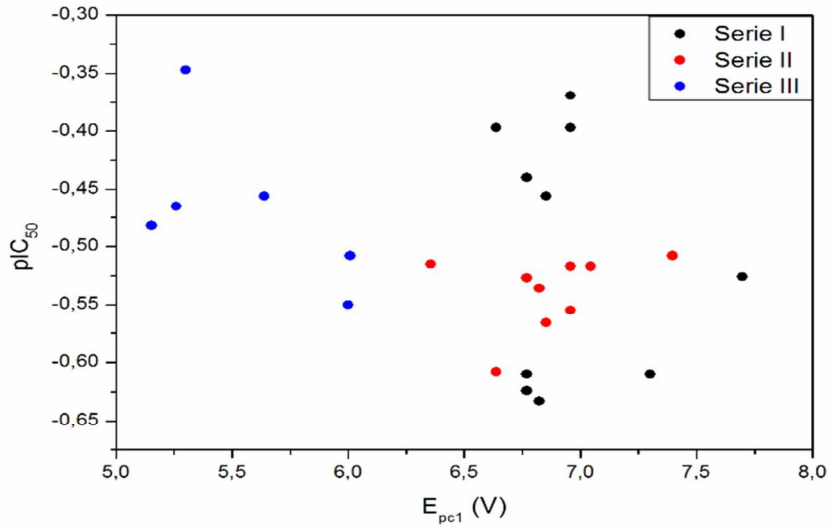

Fig. 5 Graphs correlating the values of E_{pc1} of series **I**, **II** and **III** of quinones with the trypanosomicidal effect, represented by pIC_{50}.

2.6 3D-QSAR

A 3D-QSAR-correlation analysis was performed with a set of 28 aryloxy-quinones with potent trypanosomicidal activity, selecting 19 and 9 compounds as the training and test sets, respectively. Conformational sampling on each molecule by quenched molecular dynamics and alignment by an atom-based fashion was carried out using Open3DAlign. Then, derivation of 3D-QSAR models was carried out by Partial Least-Squares (PLS) analysis with Iterative Variable Elimination (IVE-PLS) procedure by means of Open3DQSAR.[49] The statistical results for 3D-QSAR modelling gave for

RSC Advances Accepted Manuscript

internal cross-validation q^2_{LMO} of 0.75 and q^2_{LOO} of 0.78, with five components in all models. Figure 6a shows the aligned molecules and Fig. 6b the correlations between experimental versus predicted values of pIC_{50}. The correlation coefficients of our model was $R^2 = 0.99$, and standard deviation of the error of prediction (SDEP) of 0.324 for training set, as well as, the $r^2_{(pred)} = 0.94$ and SDEP of 0.115 for test set. These data indicate that a significant 3D-QSAR model was obtained.

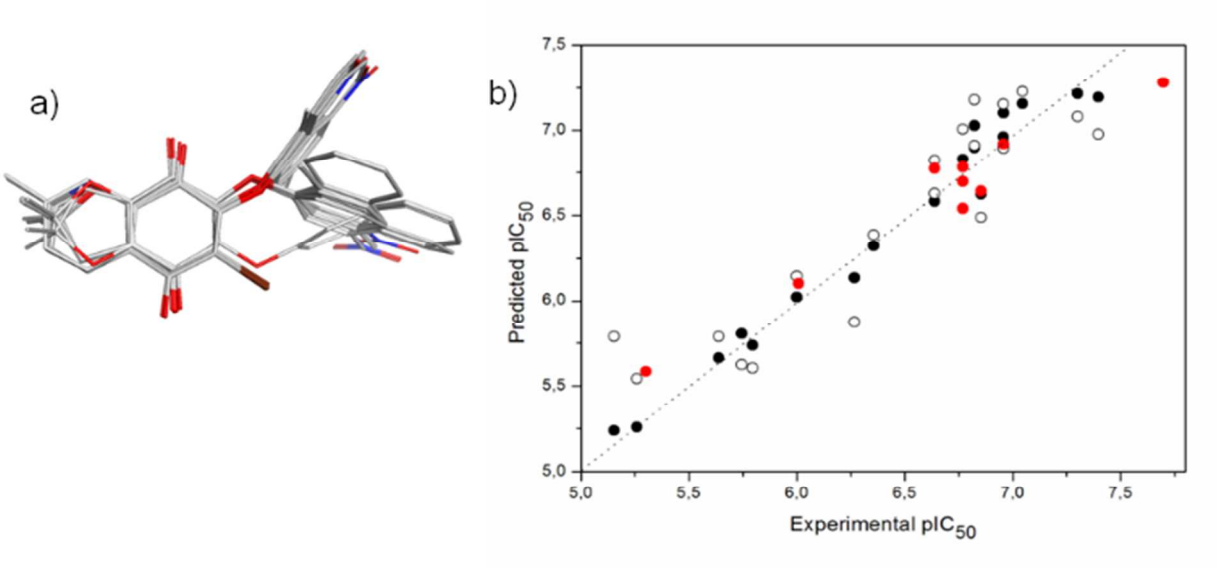

Fig. 6 a) Atom-by-atom superposition used for 3D-QSAR analysis. **b)** Scatter plot of the experimental activities versus predicted activities for 3D-QSAR model: (●) training set predictions, (○) LOO cross-validated predictions, (●) test-set predictions.

For the 3D-QSAR modeling, the contour maps were created using the data from PLS analyses. These maps help us to explain the structural features of the compounds that are contributing towards the anti-trypanosomicidal activity of the aryloxy-quinones. The steric contour map indicates the areas where the bulky substituents are predicted to increase (green) or decrease (yellow) the activity. (Fig. 7 a,b) Therefore, considering the yellow area around the aromatic moiety suggests that this ring should not have bulky groups. Furthermore, in compounds with a 2,2-dimethyl-2,3-dihydrobenzofuran system and a bromine atom at the quinone ring (**11d**, **11e**, **11h** and **11i**), the halogen substituent shifts the aryloxy group inducing an unfavorable interaction, and consequently decreases the biological activity (Fig. 7b). The electrostatic map show red contour where high electron density (negative charge) would increase the activity, and the blue contour displays areas with low electron density (partial positive charge) is expected to increase the activity (Fig. 7 c,d). The quinone ring is thought to be critical for the biological activity and the changes of its electron density might have caused an increment of the activity. The

RSC Advances Accepted Manuscript

most active compound **3b** received the influence of the NO_2 group electron-withdrawing, having a positive delocalized polar region in the aromatic ring NO_2 substituted. According to that, the electrostatic contour map (Fig. 7c) of the aromatic ring in **3b** has a positive-charge favored region. The electrostatic contour maps indicated that the positive electrostatic interaction of the aromatic ring with a possible receptor which could be increase the activity. In comparison, this interaction is lost in the less active compound **11i** (Fig. 7d).

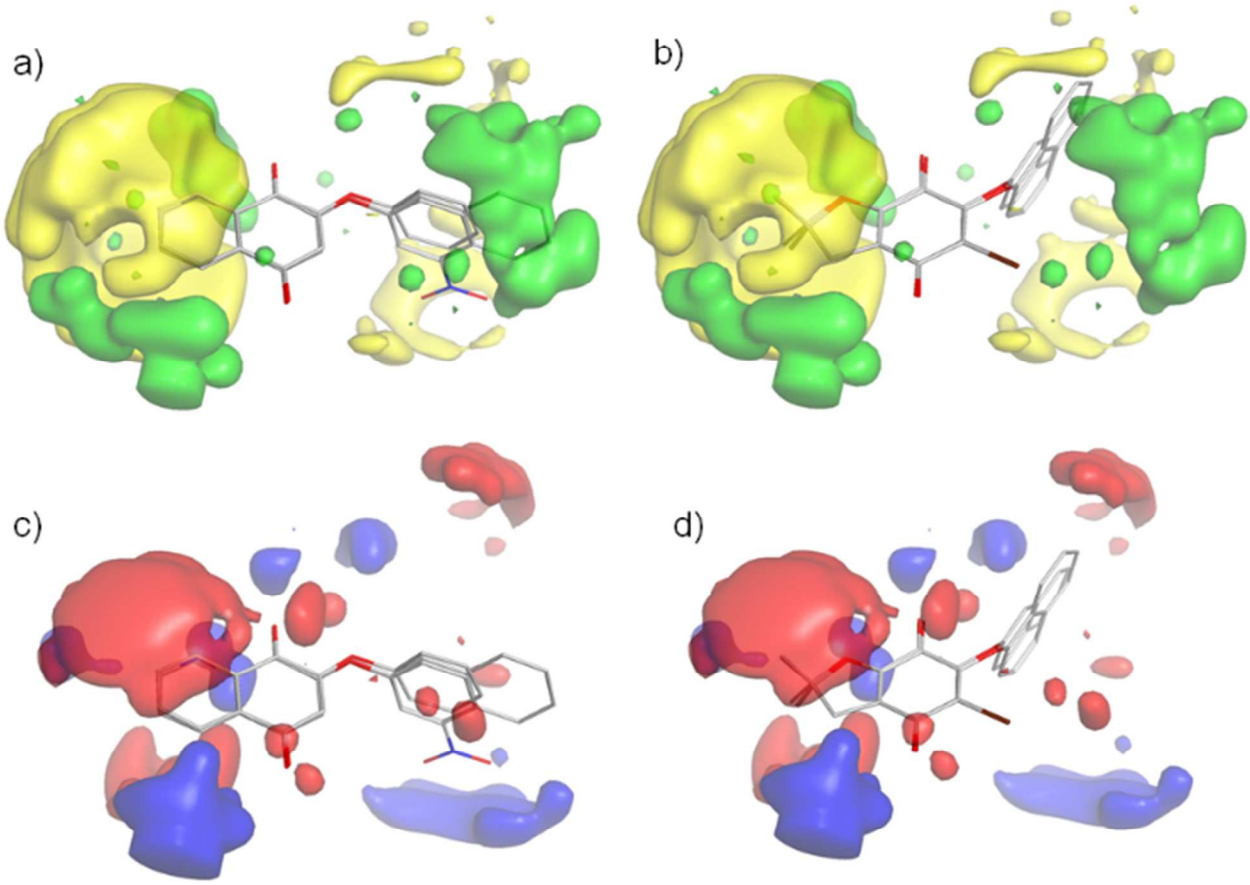

Fig. 7 a) Steric contour map for most active compounds **3a**, **3b** and **7a**. **b)** Steric contour map for least active compounds **11d**, **11h** and **11i**. **c)** Electrostatic contour map for most active compounds **3a**, **3b** and **7a**. **d)** Electrostatic contour map for least active compounds **11d**, **11h** and **11i**.

3 Conclusions

We have synthesized 27 new aryloxyquinones considering the 2-phenoxy-naphthoquinone (**3a**) as reference compound and were grouped in three series according to similar structural pattern: 2-aryloxy-naphthoquinones **3a-j**, 7-aryloxy-quinolinquinones **7a-i** and 6-aryloxy-furonaphthoquinones **11a-i**. All

RSC Advances Accepted Manuscript

compounds were evaluated as trypanosomicidal agents and tested for their unspecific cytotoxicity on murine macrophages J-774 cells. Most of these compounds were more potent than the reference drug nifurtimox *vs* epimastigote form and exhibited unprecedented selectivity against *T. cruzi* in comparison with J-774 cells, notably the 2-(3-nitrophenyloxy)-naphthoquinone **3b** (IC_{50} = 20 nM and SI = 625). Also, it was demonstrated that certain chemical modifications on the naphthoquinone moiety and on the aryloxy group, increased significantly the trypanosomicidal effect and the selectivity of some derivatives. Electrochemical studies were done in order to find out a possible structure-activity relationship and used in an attempt to understand this biological activity, but no correlation was found between the E_{pcl} and the pIC_{50}. Because of that, in *silico* studies were done through the pharmacophoric mapping and QSAR analyses. Eight out of nine molecules with the best IC_{50} and SI were chosen using the selective designed pharmacophore, proving that this procedure is able to find active and selective molecules with an enrichment factor of R = 0.99. A 3D-QSAR equation was obtained with a coefficient of determination R^2 of 0.99 and the contour maps indicated that the trypanosomicidal activity was related to the steric and electronic features in the aryloxy moiety or ring fused to the quinone system. Our current work is focused to understand in depth the selectivity and mechanism of action of the most promissory compounds.

4 Experimental

4.1 Materials and measurements

Melting points were determined on a Kofler Thermogerate apparatus and were uncorrected. Infrared spectra were recorded on a JASCO FT/IR-400 spectrophotometer. Nuclear magnetic resonance spectra were recorded, unless otherwise specified, on a Bruker AM-400 instrument using deuterochloroform solutions containing tetramethylsilane as an internal standard. Mass spectra were obtained on a HP 5988A mass spectrometer. HRMS-ESI-MS experiments were done using a Thermo Scientific Exactive Plus Orbitrap spectrometer with a constant nebulizer temperature of 250 °C. The experiments were carried out in positive ion mode, with a scan range of *m/z* 300.00-1510.40 with resolution 140.000. The samples were infused directly into the ESI source, via a syringe pump, at flow rates of 5 μL min-1, through the instrument's injection valve. Thin layer chromatography (tlc) was performed using Merck GF-254 type 60 silica gel. Column chromatography was carried out using Merck type 9385 silica gel. The purity of the compounds was determined by tlc and high-resolution mass spectrometry (HRMS).

RSC Advances Accepted Manuscript

4.2 Synthesis

General synthetic procedure of aryloxy quinones:

In a reaction flask, the suitable phenol (1 mmol) and K_2CO_3 (3 mmol) was suspended in DMF (5 ml). The mixture was stirred for 10 min, and then the corresponding quinone (1 mmol) was added. After the addition, the reaction mixture was stirred for 2-5 hours at room temperature. Later, the reaction was poured into ice water and extracted with ethyl acetate (3 x 25 mL). The combined organic layers were washed with a saturated solution of sodium sulfite (3 x 25 mL) and brine (3 x 25 mL). Finally, the organic layer was dried with anhydrous sodium sulfate and concentrated under vacuum. The solid residue was purified by column chromatography on silica gel. For compounds **3a-j**, the eluent used was dichloromethane and for **7a-i** and **11a-i** were a mixture of methanol-dichloromethane 1%.

2-phenoxynaphthalene-1,4-dione (3a). Yellow solid, yield 75%, mp 102-103 ºC (lit.[11] 101 ºC). ^{1}H NMR (400 MHz, $CDCl_3$) δ ppm: 5.99 (s, 1H), 7.15 (d, *J* = 7,7 Hz, 2H), 7.34 (t, *J* = 7,5 Hz, 1H), 7.46 (t, *J* = 7,9 Hz, 2H), 7.74-7.81 (m, 2H), 8.04-8.10 (m, 1H), 8.18-8.23 (m, 1H). ^{13}C NMR (101 MHz, $CDCl_3$) δ ppm: 113.34, 121.07 (2C), 126.18, 126.60, 126.73, 130.40 (2C), 131.06, 131.91, 133.50, 134.41, 152.67, 160.45, 179.86, 184.88. IR (KBr, cm^{-1}): 1613, 1672, 1591. HRMS-ESI for ($C_{16}H_{11}O_3$ $[M+H]^+$). Calcd: 251.0708 Found: 251.0699.

2-(3-nitrophenoxy)naphthalene-1,4-dione (3b). Yellow solid, yield 80 %, mp 170-173ºC. ^{1}H NMR (400 MHz, $CDCl_3$) δ ppm: 6.05 (s, 1H), 7.53 (dd, *J* = 1.5, 8.2 Hz, 1H), 7.69 (t, *J* = 8.2 Hz, 1H), 7.74-7.85 (m, 2H), 8.00-8.12 (m, 2H), 8.16-8.25 (m, 2H).^{13}C NMR (101 MHz, $CDCl_3$) δ ppm: 115.14, 116.53, 121.43, 126.53, 127.03, 127.23, 131.05, 131.34, 131.90, 134.00, 134.83, 149.54, 153.61, 159.31, 179.36, 184.53. IR (KBr, cm^{-1}): 1620, 1654, 1528, 1472, 1178, 1032. HRMS-ESI for ($C_{16}H_9NO_5$ $[M+H]^+$). Calcd: 296.0559 Found: 296.0560.

2-(2,5-dimethylphenoxy)naphthalene-1,4-dione (3c). Yellow oil, yield 63 %. ^{1}H NMR (400 MHz, $CDCl_3$) δ ppm: 2.15 (s, 3H), 2.33 (s, 3H), 5.83 (s, 1H), 6.86 (s, 1H), 7.02 (d, *J* = 7.6 Hz, 1H), 7.17 (d, *J* = 7.7 Hz, 1H), 7.74-7.78 (m, 2H), 8.02-8.09 (m, 1H),8.20 (dd, *J* = 6.1, 2.7 Hz, 1H). ^{13}C NMR (101 MHz, $CDCl_3$) δ ppm: 15.38, 20.98, 112.86, 121.62, 126.28, 126.67, 126.82, 127.62, 131.27, 131.80, 132.12, 133.54, 134.47, 138.07, 150.74, 159.85, 179.94, 185.14. IR (KBr, cm^{-1}): 1610, 1651, 1288, 1258, 1222. HRMS-ESI for ($C_{18}H_{14}O_3$ $[M+H]^+$). Calcd: 279.1021. Found: 279.1032.

RSC Advances Accepted Manuscript

2-bromo-3-phenoxynaphthalene-1,4-dione (3d). Yellow solid, yield 80 %, mp 160-162 °C. ^{1}H NMR (400 MHz, $CDCl_3$) δ ppm: 7.01 (d, *J* = 7.8 Hz, 2H), 7.13 (t, *J* = 7.4 Hz, 1H), 7.29-7.38 (m, 2H), 7.71-7.81 (m, 2H), 7.98-8.06 (m, 1H), 8.16-8.23 (m, 1H). ^{13}C NMR (101 MHz, $CDCl_3$) δ ppm: 116.69, 124.10, 127.35, 127.69, 129.88, 130.73, 131.17, 134.42, 134.56, 156.06, 156.41, 177.47, 178.48. IR (KBr, cm^{-1}): 1613, 1672, 1206, 1245, 1159, 1021. HRMS-ESI for ($C_{16}H_9BrO_3$ $[M+H]^+$). Calcd: 327.9735. Found: 329.1719.

2-bromo-3-(3-nitrophenoxy)naphthalene-1,4-dione (3e). Yellow solid, yield 76%, mp 197-199 °C. ^{1}H NMR (400 MHz, $CDCl_3$) δ ppm: 7.40 (ddd, *J* = 0.8, 2.5, 8.3 Hz, 1H), 7.55 (t, *J* = 8.2 Hz, 1H), 7.76-7.86 (m, 3H), 8.00-8.10 (m, 2H), 8.23-8.27 (m, 1H). ^{13}C NMR (101 MHz, $CDCl_3$) δ ppm: 111.93, 118.78, 122.78, 127.24, 127.75, 128.72, 130.28, 130.63, 131.28, 134.36, 134.59, 149.49, 155.25, 156.52, 176.92, 177.76. IR (KBr, cm^{-1}): 1677, 1536, 1349, 1245, 1018. HRMS-ESI for ($C_{16}H_9BrNO_5$ $[M+H]^+$). Calcd: 373.9664. Found: 373.9648.

2-bromo-3-(2,5-dimethylphenoxy)naphthalene-1,4-dione (3f). Orange solid, yield 97 %, mp 196-198 °C. ^{1}H NMR (400 MHz, $CDCl_3$) δ ppm: 2.22 (s, 3H), 2.38 (s, 3H), 6.48 (s, 1H), 6.86 (d, *J* = 7.6 Hz, 1H), 7.15 (d, *J* = 7.6 Hz, 1H), 7.68-7.81 (m, 2H), 7.98-8.09 (m, 1H), 8.18-8.27 (m, 1H). ^{13}C NMR (101 MHz, $CDCl_3$) δ ppm: 15.79, 20.90, 115.94, 124.68, 124.95, 125.11, 126.75, 127.26, 127.55, 128.21, 131.30, 134.25, 134.43, 136.83, 154.82, 156.76, 177.54, 178.51. IR (KBr, cm^{-1}): 1679, 199, 1244, 1098, 1002. HRMS-ESI for ($C_{18}H_{13}BrO_3$ $[M+Na^+]^+$). Calcd: 380.9925 Found: 381.2984**.**

2-(naphthalen-2-yloxy)naphthalene-1,4-dione (3g). Yellow solid, yield 95%, mp 163-164 °C. ^{1}H NMR (400 MHz, $CDCl_3$) δ ppm: 6.01 (s, 1H), 7.27 (dd, *J* = 2.4, 8.8 Hz, 1H), 7.48-7.57 (m, 2H), 7.60 (d, *J* = 2.3 Hz, 1H), 7.75 (dd, *J* = 2.8, 5.5 Hz, 2H), 7.80-7.84 (m, 1H), 7.87-7.90 (m, 1H), 7.94 (d, *J* = 8.9 Hz, 1H), 8.02-8.07 (m, 1H), 8.18-8.22 (m, 1H). ^{13}C NMR (101 MHz, $CDCl_3$) δ ppm: 113.73, 118.35, 120.11, 126.28, 126.37, 126.84, 127.18, 127.72, 128.02, 130.80, 131.18, 131.74, 132.03, 133.58, 134.07, 134.49, 150.29, 160.58, 179.95, 184.90. IR (KBr, cm-1): 1629, 1671, 1242. HRMS-ESI for ($C_{20}H_{12}O_3$ $[M+H]^+$). Calcd: 301.0865. Found: 301.0865.

2-bromo-3-(naphthalene-2-yloxy)naphthalene-1,4-dione (3h). Orange solid, yield 67 %, mp 166-168 °C. ^{1}H NMR (400 MHz, $CDCl_3$) δ ppm: 7.27 – 7.22 (m, 1H), 7.33 (dd, *J* = 8.9, 2.5 Hz, 1H), 7.42 (m, 2H), 7.67 (d, *J* = 7.8 Hz, 1H), 7.74 (m, 2H), 7.81 (d, *J* = 7.9 Hz, 1H), 7.84 (d, *J* = 8.9 Hz, 1H), 8.01 (dd, *J* = 7.4, 1.3 Hz, 1H), 8.24 – 8.20 (m, 1H). ^{13}C NMR (101 MHz, $CDCl_3$) δ ppm: 111.78, 117.98, 125.13, 126.91, 127.19, 127.35, 127.69, 127.89, 128.01, 130.21, 130.49, 130.67, 131.16, 133.92,

RSC Advances Accepted Manuscript

134.40, 134.54, 154.15, 156.16, 177.39, 178.49. IR (KBr, cm^{-1}): 1671, 1509, 1572, 1195, 1158. HRMS-ESI for ($C_{20}H_{11}BrO_3$ $[M+Na^+]^+$). Calcd: 400.9789 Found: 400.9766.

2-(naphthalen-1-yloxy)naphthalene-1,4-dione (3i). Yellow solid, yield 53%, mp 156-158 °C. ^1H NMR (400 MHz, $CDCl_3$) δ ppm: 5.82 (s, 1H), 7.27 (d, *J* = 7.3 Hz, 1H), 7.45-7.59 (m, 3H), 7.71 – 7.79 (m, 2H), 7.81 (d, *J* = 8.3 Hz, 1H), 7.86 (d, *J* = 8.1 Hz, 1H), 7.92 (d, *J* = 8.0 Hz, 1H), 8.03 (br, 1H), 8.24 (br, 1H). ^{13}C NMR (101 MHz, $CDCl_3$) δ ppm: 113.78, 117.63, 121.24, 125.75, 126.05, 126.33, 126.89, 126.93, 127.12, 127.16, 128.36, 131.27, 132.10, 133.64, 134.53, 135.21, 148.64, 160.62, 179.91, 185.00. IR (KBr, cm^{-1}): 1602, 1682, 1034, 1248. HRMS-ESI for ($C_{20}H_{12}O_3$ $[M+H]^+$). Calcd: 301.0865 Found: 301.0859.

2-bromo-3-(naphthalen-1-yloxy)naphthalene-1,4-dione (3j). Red solid, yield 59%, mp 161-163 °C. ^1H NMR (400 MHz, $CDCl_3$) δ ppm: 6.74 (d, *J* = 7.5 Hz, 1H), 7.25 (t, *J* = 7.9 Hz, 1H), 7.52–7.65 (m, 3H), 7.67–7.79 (m, 2H), 7.86 (d, *J* = 6.9 Hz, 1H), 7.97 (d, *J* = 7.6 Hz, 1H), 8.20 (d, *J* = 8.3 Hz, 1H), 8.34 (d, *J* = 7.5 Hz, 1H). ^{13}C NMR (101 MHz, $CDCl_3$) δ ppm: 109.60, 121.99 (2C), 124.15, 125.22, 126.48, 127.09, 127.37, 127.72, 127.81, 130.72 (2C), 131.21, 134.43, 134.57, 134.97, 152.56, 156.74, 177.27, 178.51. IR (KBr, cm^{-1}): 1682, 1601, 1570, 1247, 1221. HRMS-ESI for ($C_{20}H_{11}BrO_3$ $[M+Na^+]^+$). Calcd: 400.9789. Found: 400.9771.

7-phenoxyquinoline-5,8-dione (7a). Yellow solid, yield 47 %, mp 172-173 °C. ^1H NMR (400 MHz, $CDCl_3$) δ ppm: 6.04 (s, 1H), 7.19–7.13 (m, 2H), 7.34 (t, *J* = 7.5 Hz, 1H), 7.49 (t, *J* = 8.0 Hz, 2H), 7.72 (dd, *J* = 4.7, 7.9 Hz, 1H), 8.41 (dd, *J* = 1.7, 7.9 Hz, 1H), 9.07 (dd, *J* = 1.7, 4.7 Hz, 1H). ^{13}C NMR (101 MHz, $CDCl_3$) δ ppm: 112.78, 115.50, 121.08, 126.95, 128.18, 129.06, 129.61, 130.58, 134.46, 147.00, 152.52, 154.55, 161.10, 178.05, 183.73. IR (KBr, cm^{-1}): 3052, 3016, 1610, 1280, 1240, 1083. HRMS-ESI for ($C_{15}H_9NO_3$ $[M+H]^+$). Calcd: 252.0661. Found: 252.0654.

7-(2,5-dimethylphenoxy)quinoline-5,8-dione (7b). Orange solid, yield 63 %, mp 177-179 °C. ^1H NMR (400 MHz, $CDCl_3$) δ ppm: 2.16 (s, 3H), 2.35 (s, 3H), 5.91 (s, 1H), 6.87 (s, 1H), 7.04 (d, *J* = 7.8 Hz, 1H), 7.19 (d, *J* = 7.8 Hz, 1H), 7.72 (dd, *J* = 4.7, 7.9 Hz, 1H), 8.41 (dd, *J* = 1.7, 7.9 Hz, 1H), 9.07 (dd, *J* = 1.7, 4.7 Hz, 1H). ^{13}C NMR (101 MHz, $CDCl_3$) δ ppm: 183.84, 178.01, 160.37, 154.47, 150.52, 147.04, 138.18, 134.44, 131.86, 129.10, 128.15, 127.83, 126.53, 121.45, 112.26, 20.95, 15.34. IR (KBr, cm^{-1}): 1654, 1613, 1244, 1141. HRMS-ESI for ($C_{17}H_{13}NO_3$ $[M+H]^+$). Calcd: 280.0974. Found: 280.0968.

RSC Advances Accepted Manuscript

2-methyl-7-phenoxyquinoline-5,8-dione (7c). Yellow solid, yield 49%, mp 165-167. ^{1}H NMR (400 MHz, $CDCl_3$) δ ppm: 2.80 (s, 3H), 5.98 (s, 1H), 7.15 (d, *J* = 7.6 Hz, 2H), 7.32 (d, *J* = 7.2 Hz, 1H), 7.48 (t, *J* = 7.9 Hz, 2H), 7.55 (d, *J* = 8.0 Hz, 1H), 8.27 (d, *J* = 8.0 Hz, 1H). ^{13}C NMR (101 MHz, $CDCl_3$) δ ppm: 25.60, 112.88, 121.49 (2C), 127.17, 127.27, 128.44, 130.84 (2C), 134.85, 146.88, 152.98, 161.27, 165.21, 178.63, 184.27. IR (KBr, cm^{-1}): 1640, 1614, 1582, 1289, 1226. HRMS-ESI for ($C_{16}H_{11}NO_3$ $[M+H]^+$) Calcd: 266.0817. Found: 266.0810.

2-methyl-7-(3-nitrophenoxy)quinoline-5,8-dione (7d). Yellow solid, yield 24 %, mp 197-198°C. ^{1}H NMR (400 MHz, $CDCl_3$) δ ppm: 2.81 (s, 3H), 6.06 (s, 1H), 7.54 (d, *J* = 8.1 Hz, 1H), 7.58 (d, *J* = 8.1 Hz, 1H), 7.70 (t, *J* = 8.2 Hz, 1H), 8.05 (s, 1H), 8.22 (d, *J* = 8.2 Hz, 1H), 8.29 (d, *J* = 8.0 Hz, 1H). ^{13}C NMR (101 MHz, $CDCl_3$) δ ppm: 183.52, 177.72, 165.38, 159.71, 153.38, 149.56, 146.44, 134.71, 131.44, 128.41, 127.36, 126.94, 121.66, 116.65, 114.06, 25.37. IR (KBr, cm^{-1}): 1698, 1654, 1350, 1258, 1163. HRMS-ESI for ($C_{16}H_{10}N_2O_5$ $[M+H]^+$) Calcd: 311.0668. Found: 311.0663.

7-(2,5-dimethylphenoxy)-2-methylquinoline-5,8-dione (7e). Yellow solid, yield 92 %, mp 165-166°C. ^{1}H NMR (400 MHz, $CDCl_3$) δ ppm: 2.15 (s, 3H), 2.34 (s, 3H), 2.80 (s, 3H), 5.85 (s, 1H), 6.86 (s, 1H), 7.03 (d, *J* = 7.7 Hz, 1H), 7.18 (d, *J* = 7.7 Hz, 1H), 7.56 (d, *J* = 8.0 Hz, 1H), 8.27 (d, *J* = 8.0 Hz, 1H). ^{13}C NMR (101 MHz, $CDCl_3$) δ ppm: 15.28, 20.90, 25.20, 111.95, 121.49, 126.51, 126.92, 127.68, 128.05, 131.77, 134.47, 138.05, 146.53, 150.57, 160.11, 164.74, 178.21, 183.98. IR (KBr, cm^{-1}): 1652, 1322, 1114, 1110. HRMS-ESI for ($C_{18}H_{15}NO_3$ $[M+H]^+$) Calcd: 294.1130. Found: 294.1121.

7-(naphthalen-2-yloxy)quinoline-5,8-dione (7f). Yellow solid, yield 42 %, mp 190-191 °C. ^{1}H NMR (400 MHz, $CDCl_3$) δ ppm: 6.07 (s, 1H), 7.27 (d, *J* = 9.3 Hz, 1H), 7.54 (m, 2H), 7.61 (s, 1H), 7.71 (dd, *J* = 5.1, 7.2 Hz, 1H), 7.79-7.93 (m, 2H), 7.96 (d, *J* = 8.9 Hz, 1H), 8.39 (d, *J* = 7.8 Hz, 1H), 9.07 (d, *J* = 3.7 Hz, 1H). ^{13}C NMR (101 MHz, $CDCl_3$) δ ppm: 113.03, 118.43, 119.92, 126.54, 127.31, 127.77, 128.06, 128.18, 129.07, 130.96, 131.84, 134.04, 134.45, 147.02, 150.02, 154.57, 161.16, 178.09, 183.67. IR (KBr, cm^{-1}): 1649, 1222, 1003. HRMS-ESI for ($C_{19}H_{11}NO_3$ $[M+H]^+$) Calcd: 301.0739. Found: 302.0809.

2-methyl-7-(naphthalen-2-yloxy)quinoline-5,8-dione (7g). Yellow solid, yield 33 %, mp 198-199 °C. ^{1}H NMR (400 MHz, $CDCl_3$) δ ppm: 2.80 (s, 3H), 6.01 (s, 1H), 7.24-7.30 (m, 1H), 7.49-7.58 (m, 3H), 7.60 (d, *J* = 1.7 Hz, 1H), 7.79-7.91 (m, 2H), 7.93 (t, *J* = 8.7 Hz, 1H), 8.25 (d, *J* = 8.0 Hz, 1H). ^{13}C NMR (101 MHz, $CDCl_3$) δ ppm: 25.25, 112.76, 118.43, 120.02, 126.44, 126.92, 127.22, 127.72, 128.01, 128.11, 130.84, 131.77, 134.01, 134.49, 146.52, 150.11, 160.95, 164.85, 178.27, 183.83. IR

RSC Advances Accepted Manuscript

(KBr, cm^{-1}): 1696, 1586, 1283, 1176. HRMS-ESI for ($C_{20}H_{13}NO_3$ $[M+H]^+$) Calcd: 316.0974. Found: 316.0964.

7-(naphthalen-1-yloxy)quinoline-5,8-dione (7h). Yellow solid, yield 24 %, mp 118-120°C. ^1H NMR (400 MHz, $CDCl_3$) δ ppm: 6.07 (s, 1H), 7.27 (dd, *J* = 1.6, 8.9 Hz, 1H), 7.54 (m, 2H), 7.61 (d, *J* = 1.7 Hz, 1H), 7.71 (dd, *J* = 4.7, 7.8 Hz, 1H), 7.81-7.85 (m, 1H), 7.88-7.92 (m, 1H), 7.96 (d, *J* = 8.9 Hz, 1H), 8.39 (d, *J* = 7.9 Hz, 1H), 9.07 (d, *J* = 4.6 Hz, 1H). ^{13}C NMR (101 MHz, $CDCl_3$) δ ppm: 113.01, 118.43, 119.92, 126.54, 127.31, 127.76, 128.05, 128.19, 129.06, 130.96, 131.83, 134.03, 134.45, 147.01, 149.99, 154.57, 161.16, 178.09, 183.67. IR (KBr, cm^{-1}): 1656, 1609, 1242. HRMS-ESI for ($C_{19}H_{11}NO_3$ $[M]^-$) Calcd: 300.0666. Found: 300.0656.

2-methyl-7-(naphthalen-1-yloxy)quinoline-5,8-dione (7i). Yellow solid, yield 25 %, mp 199-200 °C. ^1H NMR (400 MHz, $CDCl_3$) δ ppm: 2.18 (s, 3H), 6.43 (s, 1H), 6.82 (d, *J* = 7.6 Hz, 1H), 7.10 (d, *J* = 7.6 Hz, 1H), 7.69 – 7.75 (m, 3H), 7.98 (d, *J* = 7.2 Hz, 1H), 8.14 – 8.18 (m, 2H). ^{13}C NMR (101 MHz, $CDCl_3$) δ ppm: 15.79, 115.93, 124.68, 124.94, 126.72, 127.26, 127.55, 128.21, 130.65, 131.16, 131.29, 134.22, 134.40, 134.51, 136.79, 142.58, 154.81, 156.76, 177.54, 178.56. IR (KBr, cm^{-1}): 1653, 1615, 1225. HRMS-ESI for ($C_{20}H_{13}NO_3$ $[M]^-$) Calcd: 314.0823 Found: 314.0814.

2,2-dimethyl-6-phenoxy-2,3-dihydrobenzofuran-4,7-dione (11a). Orange oil, yield 47 %. ^1H NMR (400 MHz, $CDCl_3$) δ ppm: 1.56 (s, 6H), 2.92 (s, 2H), 5.47 (s, 1H), 7.08 (d, *J* = 7.8 Hz, 2H), 7.30 (d, *J* = 7.4 Hz, 1H), 7.44 (t, *J* = 7.8 Hz, 2H). ^{13}C NMR (101 MHz, $CDCl_3$) δ ppm: 28.44 (2C), 39.63, 93.44, 107.71, 117.94, 121.06 (2C), 126.79, 130.45 (2C), 153.02, 158.61, 161.13, 178.42, 180.24. IR (KBr, cm^{-1}): 2923, 1653, 1249, 1207. HRMS-ESI for ($C_{16}H_{14}O_4$ $[M+H]^+$) Calcd: 271.0970. Found: 271.0978.

2,2-dimethyl-6-(3-nitrophenoxy)-2,3-dihydrobenzofuran-4,7-dione (11b). Orange-red oil, yield 26 %. ^1H NMR (400 MHz, $CDCl_3$) δ ppm: 1.58 (s, 6H), 2.94 (s, 2H), 5.55 (s, 1H), 7.48 (d, *J* = 9.0 Hz, 1H), 7.67 (t, *J* = 8.2 Hz, 1H), 7.99 (s, 1H), 8.18 (d, *J* = 8.2 Hz, 1H). ^{13}C NMR (101 MHz, $CDCl_3$) δ ppm: 28.34 (2C), 39.46, 93.70, 109.18, 116.43, 118.32, 121.42, 127.15, 131.26, 149.41, 153.65, 158.44, 159.65, 177.53, 179.55. IR (KBr, cm^{-1}): 1613, 1535, 1203. HRMS-ESI for ($C_{16}H_{13}NO_6$ $[M+H]^+$) Calcd: 316.0821. Found: 316.0792.

6-(2,5-dimethylphenoxy)-2,2-dimethyl-2,3-dihydrobenzofuran-4,7-dione (11c). Orange-red oil, yield 50 %. ^1H NMR (400 MHz, $CDCl_3$) δ ppm: 1.57 (s, 6H), 2.13 (s, 3H), 2.31 (s, 3H), 2.92 (s, 2H), 5.34 (s, 5H), 6.79 (s, 1H), 6.99 (d, *J* = 7.6 Hz, 1H), 7.14 (d, *J* = 7.7 Hz, 1H). ^{13}C NMR (101 MHz, $CDCl_3$) δ ppm: 15.25, 20.85, 28.31 (2C), 39.47, 93.25, 107.03, 117.76, 121.31, 126.34, 127.52, 131.63,

RSC Advances Accepted Manuscript

137.88, 150.91, 158.51, 160.28, 178.24, 180.21. IR (KBr, cm^{-1}): 1659, 1589, 1104. HRMS-ESI for ($C_{18}H_{18}O_4$ $[M+H]^+$) Calcd: 299.1283. Found: 299.1273.

5-bromo-2,2-dimethyl-6-phenoxy-2,3-dihydrobenzofuran-4,7-dione (11d). Red solid, yield 50% mp 140-142 °C. ^{1}H NMR (400 MHz, $CDCl_3$) δ ppm: 1.56 (s, 6H), 2.84 (s, 2H), 6.97 (d, *J* = 7.8 Hz, 2H), 7.12 (t, *J* = 7.4 Hz, 1H), 7.28-7.36 (m, 2H), ^{13}C NMR (101 MHz, $CDCl_3$) δ ppm: 28.45 (2C), 39.5, 93.95, 116.85 (2C), 118.85, 120.31, 124.14, 129.90 (2C), 155.11, 156.66, 157.54, 173.37, 176.15. IR (KBr, cm^{-1}): 1653, 1588, 1282. HRMS-ESI for ($C_{16}H_{13}BrO_4$ [M]) Calcd: 347.9997. Found: 348.0137.

5-bromo-2,2-dimethyl-6-(3-nitrophenoxy)-2,3-dihydrobenzofuran-4,7-dione (11e). Red solid, yield 57 %, mp 177-179 °C. ^{1}H NMR (400 MHz, $CDCl_3$) δ ppm: 1.58 (s, 6H), 2.87 (s, 2H), 7.36 (ddd, *J* = 0.9, 2.5, 8.3 Hz, 1H), 7.52 (t, *J* = 8.2 Hz, 1H), 7.76 (t, *J* = 2.3 Hz, 1H), 8.00 (ddd, *J* = 0.9, 2.1, 8.2 Hz, 1H). ^{13}C NMR (101 MHz, $CDCl_3$) δ ppm: 28.46 (2C), 39.50, 94.34, 111.84, 118.98, 119.04, 121.38, 123.24, 130.63, 149.26, 154.06, 156.75, 157.73, 172.82, 175.57. IR (KBr, cm^{-1}): 1693, 1647, 1577, 1552, 1268, 1243. HRMS-ESI for ($C_{16}H_{12}BrNO_6$ $[M+H]^+$) Calcd: 393.9926. Found: 393.9908.

5-bromo-6-(2,5-dimethylphenoxy)-2,2-dimethyl-2,3-dihydrobenzofuran-4,7-dione (11f). Orange solid, yield 83%, mp 146-147 °C. ^{1}H NMR (400 MHz, $CDCl_3$) δ ppm: 1.56 (s, 6H), 2.26 (s, 3H), 2.33 (s, 3H), 2.84 (s, 2H), 6.47 (s, 1H), 6.84 (d, *J* = 7.6 Hz, 1H), 7.10 (d, *J* = 7.6 Hz, 1H). ^{13}C NMR (101 MHz, $CDCl_3$) δ ppm: 15.84, 21.24, 28.31, 39.53, 93.74, 116.31, 118.51, 119.06, 121.41, 124.81, 125.05, 131.34, 136.84, 155.13, 155.73, 157.48, 173.41, 176.23. IR (KBr, cm^{-1}): 1674, 1656, 1570, 1207. HRMS-ESI for ($C_{18}H_{17}BrO_4$ $[M+H]^+$) Calcd: 377.0388. Found: 379.0361.

2,2-dimethyl-6-(naphthalen-2-yloxy)-2,3-dihydrobenzofuran-4,7-dione (11g). Orange-red oil, yield 25 %. ^{1}H NMR (400 MHz, $CDCl_3$) δ ppm: 1.56 (s, 6H), 2.94 (s, 2H), 5.51 (s, 1H), 7.20 (d, *J* = 8.9 Hz, 1H), 7.52 (dd, *J* = 4.1, 7.4 Hz, 3H), 7.80 (d, *J* = 7.1 Hz, 1H), 7.86 (d, *J* = 8.1 Hz, 1H) 7.91 (d, J = 8.9 Hz, 1H). ^{13}C NMR (101 MHz, $CDCl_3$) δ ppm: 28.41 (2C), 39.61, 93.43, 107.98, 117.96, 118.28, 119.99, 126.44, 127.23, 127.74, 128.04, 130.75, 131.77, 134.02, 150.51, 158.62, 161.11, 178.39, 180.13. IR (KBr, cm^{-1}): 1672, 1594, 1197. HRMS-ESI for ($C_{20}H_{16}O_4$ $[M+H]^+$) Calcd: 321.1127. Found: 321.1127.

5-bromo-2,2-dimethyl-6-(naphthalene-2-yloxy)-2,3-dihydrobenzofuran-4,7-dione (11h). Red solid, yield 47 %, mp 182-183°C. ^{1}H NMR (400 MHz, $CDCl_3$) δ ppm: 1.63 (s, 6H), 3.01 (s, 2H), 7.62 (d, *J* = 8.9 Hz, 3H), 7.71 (t, *J* = 8.3 Hz, 1H), 7.85-7.97 (m, 2H), 9.50 (d, *J* = 8.4 Hz, 1H). ^{13}C NMR (101 MHz, $CDCl_3$) δ ppm: 28.56 (2C), 40.20, 93.10, 112.51, 119.63, 121.31, 125.92, 126.80 127.95, 128.09,

RSC Advances Accepted Manuscript

128.20, 129.08, 131.59, 132.05, 150.68, 156.04, 156.92, 169.03, 180.24. IR (KBr, cm^{-1}): 1681, 1647, 1341. HRMS-ESI for ($C_{20}H_{15}BrO_4$ $[M+H]^+$) Calcd: 399.0232. Found: 399.2946

5-bromo-2,2-dimethyl-6-(naphthalene-1-yloxy)-2,3-dihydrobenzofuran-4,7-dione (11i). Orange solid, yield 42%, mp 179-180 °C. ^{1}H NMR (400 MHz, $CDCl_3$) δ: 1.61 (s, 6H), 2.98 (s, 2H), 7.26 (br, 1H), 7.61 – 7.71 (m, 2H), 7.81 (d, *J* = 8.7 Hz, 1H), 7.96 (d, *J* = 7.8 Hz, 1H), 8.11 (d, *J* = 8.7 Hz, 1H), 8.43 (d, *J* = 7.8 Hz, 1H). ^{13}C NMR (101 MHz, $CDCl_3$) δ 28.40, 39.64, 93.06, 119.26, 119.60, 121.07, 121.15, 127.29 (2C), 127.59 (2C), 127.94 (2C), 128.70 (2C), 133.73, 157.87, 168.96 178.49, 180.85. IR (KBr, cm^{-1}): 1793, 1650, 1370. HRMS-ESI for ($C_{20}H_{15}BrO_4$ $[M+H]^+$) Calcd: 399.0232. Found: 399.1966.

4,5,6-tribromo-2,2-dimethyl-2,3-dihydrobenzofuran-7-ol (9b). To a solution of 2,3-dihydro-2,2-dimethyl-7-benzofuranol (1 mmol) in chloroform (30 mL), under magnetic stirring at room temperature, was added dropwise a solution of bromine (5 mmol) in chloroform (15 mL) . The mixture was stirred for 1.5 hour and then was washed with sodium thiosulfate solution (3 x 15 mL) and water (3 x 15 mL). The organic extract was dried over anhydrous sodium sulfate filtered and concentrated. The crude was purified on silica gel column using dichloromethane as eluent. White solid, yield 57%, mp 120 -121 °C. ^{1}H NMR (400 MHz, $CDCl_3$) δ ppm: 1.53 (s, 6H), 3.07 (s,1H), 5.43 (s, 2H). ^{13}C NMR (101 MHz, $CDCl_3$) δ ppm: 28.40 (2C), 46.46, 89.51, 112.40, 112.85, 116.10, 130.07, 138.14, 145.10.

5,6-dibromo-2,2-dimethyl-2,3-dihydrobenzofuran-4,7-dione (10b). A solution of chromium oxide (2 mmol) in water (4 mL) was added dropwise at room temperature to a solution containing the compound **9b** (0.5 mmol) in 9 ml of a mixture of glacial acetic acid/water (3.5/1). The mixture was stirred for two hours and then water (20 mL) was added and extracted with CH_2Cl_2. The organic phase was washed with sodium bicarbonate solution 10% until neutral, dried with anhydrous sodium sulfate filtered and concentrated. The crude was purified on silica gel column using dichloromethane as eluent. Red solid, yield 63%, mp 108-110 °C. ^{1}H NMR (400 MHz, $CDCl_3$) δ ppm: 1.57 (s, 6H), 2.94 (s, 2H). ^{13}C NMR (101 MHz, $CDCl_3$) δ ppm: 28.23, 40.09, 46.47, 93.76, 120.27, 135.25, 141.46, 156.97, 170.58, 174.36. IR (KBr, cm^{-1}): 1639, 1684, 1177, 762. HRMS-ESI for ($C_{10}H_8Br_2O_3$ $[M+H]^+$) Calcd: 334.8918. Found: 336.8887.

4.3 Biology

T. cruzi Y strain epimastigotes were grown at 28 °C in an axenic medium (BHI-tryptose) as previously described,[25, 26] complemented with 5% foetal bovine serum. Epimastigotes from a 10-day-old culture

RSC Advances Accepted Manuscript

(stationary phase) were inoculated into 50 mL of fresh culture medium to reach an initial concentration of 1×10^6 cells/mL. Cell growth was monitored by measuring the absorbance of the culture at 600 nm every day. Before inoculation, the media was supplemented with a given amount of the drug from a stock solution in DMSO (25 mM). The final DMSO concentration in the culture medium never exceeded 0.4%, and the control was run in the presence of 0.4% DMSO and in the absence of drugs. The percentage of inhibition (%GI) and IC_{50} values, 50% inhibitory concentrations, parasite growth was followed in the absence (control) and in the presence of a range of concentrations of the corresponding drug. On day 5, the absorbance of the culture was measured and related to the control. The IC_{50} value was taken as the concentration of drug needed to reduce the absorbance ratio to 50%.[25, 26] J-774 murine macrophage-like cells (ATCC, USA) were maintained by passage in Dulbecco's modified Eagle's medium (DMEM) containing 4 mM L-glutamine, and supplemented with 10% heat inactivated foetal calf serum and 1% of antibiotics (10.000 U/mL penicillin and 10.000 U/mL streptomycin). J-774 cells were seeded (1×10^5 cells/well) in 96 well microplates with 200 mL of RPMI 1640 medium supplemented with 20% heat-inactivated foetal calf serum. Cells were allowed to attach for 48 h in a humidified 5% CO_2/95% air atmosphere at 37 °C and, then, exposed to compounds (100.0 to 400.0 μM) for 48 h. Afterward, cell viability was assessed by measuring the mitochondrial-dependent reduction of MTT (Sigma) to formazan. For that purpose, MTT was added to cells to a final concentration 0.4 mg/mL and cells were incubated at 37 °C for 3 h. After removing the media, formazan crystals were dissolved in DMSO (0.18 mL), and the absorbance at 595 nm was read using a microplate spectrophotometer. Results are expressed as IC_{50} (compound concentration that reduce 50% control absorbance at 595 nm).[25] Every IC_{50} is the average of three independent experiments. The selectivity index, SI, was expressed as the ratio between IC_{50} in macrophages and IC_{50} in *T. cruzi* (Y strain).

4.4 Pharmacophore

The 3D-structure of the pharmacophore hypothesis was carried out using "Molecular Operating Environment (MOE) software version 2013-2014", Chemical Computing Group INC., 1010 Sherbrook Street West, Suite 910, Montreal, H3A 2R7, Canada.

4.5 3D-QSAR

The data set was split into a 19 compounds as training set (2/3 of the compounds) and 9 compounds as test set (1/3 of the compounds). Alignments were carried out in an atom-by-atom based on a

RSC Advances Accepted Manuscript

Conformational sampling by quenched molecular dynamics was carried out using Open3Daling[50] on each structure (MMFF94 force-field, GB/SA implicit solvent model, 1000 5 ps molecular dynamics runs at 1000 K followed by energy minimization), keeping the most stable conformations in a 8 kcal/mol^{-1} range from the global minimum; this energy strain threshold was previously shown to include a percentage of experimentally found bioactive. The aligned ligand ensembles were enclosed in a grid box exceeding the largest molecule by 5 Å in each direction; a 1 Å step size was preferred to the original coarser 2 Å mesh to reduce the dependency from grid-to-molecule reciprocal orientations. Steric and electrostatic MIFs were computed with Open3DQSAR using MMFF94 van der Waals parameters and charges. The probe was constituted by a sp^3 carbon atom bearing a unit positive charge. Training set MIF data were pre filtered an energy cut-off was set at (30 kcal/mol; variables having a standard deviation below 2.0 were discarded; block unscaled weighting was applied to steric and electrostatic fields to give them the same importance in the PLS model. pIC_{50} values corresponding to the individual molecules were correlated with MIF data for each alignment using PLS regression; the optimal number of principal components (PC) to be extracted was chosen with the same criterion adopted by Tosco *et al.*,[51] namely the one giving rise to the best leave-one-out cross-validation performance, expressed as q^2_{LOO}. Finally, the predictive power of each PLS model was evaluated against the external test set and expressed both as r^2_{pred} and as standard deviation of the error of prediction (SDEP).

4.6 Electrochemical studies

The cyclic voltammetry experiments were carried out with a CH Instruments (USA) model 620C potentiostat, the scan rate was 50 mVs^{-1}. A three-electrode system consisting of a working glassy carbon electrode, 3 mm diameter, an Ag/AgCl reference electrode (3 M KCl), and a platinum wire auxiliary electrode. The glassy carbon electrode was cleaned up by polishing with alumina on a polishing felt (BAS polishing kit). All experiments were conducted at room temperature (25 ± 2 ºC) and purging with nitrogen. The compounds (1.0 mM) were dissolved in 0.1 M tetrabutylammonium perchlorate (TBAP) in dimethylformamide (DMF).

Acknowledgements

We are grateful to Fondecyt (Grants 1110749 and 1120128), KV thanks to PROMEP-México (Grant 103.5 /10/5345), CSIC-UdelaR (Proyecto Grupos Nº 661) of Uruguay, MP is grateful to the

RSC Advances Accepted Manuscript

PEDECIBA-UDelaR Master in Bioinformatics. JV and EB thank ANII (Uruguay) for their scholarships. JSD acknowledges support from Post-Doctoral fellow Fondecyt (Grant 3130359).

Notes and references

1. P. J. Hotez, *PLoS Negl. Trop. Dis.*, 2007, **1**, e149.
2. S. P. Montgomery, M. C. Starr, P. T. Cantey, M. S. Edwards and S. K. Meymandi, *Am. J. Trop. Med. Hyg.*, 2014, **90**, 814.
3. L. Rodriguez-Guerineau, K. M. Posfay-Barbe, M. Monsonis-Cabedo, T. Juncosa-Morros, A. Diana, C. A. Wyler-Lazarevic, B. M. de Tejada, F. Chappuis, V. Fumado-Perez and Y. Jackson, *Pediatr. Infect. Dis. J.*, 2014, **33**, 458.
4. A. Pinto, S. Pett and Y. Jackson, *Aust. Fam. Physician*, 2014, **43**, 440.
5. W. R. Steele, E. H. Hewitt, A. M. Kaldun, D. E. Krysztof, R. Y. Dodd and S. L. Stramer, *Transfusion*, 2014, **54**,2092.
6. www.who.int/neglected_disease/disease/chagas/en.
7. L. Murcia, B. Carrilero and M. Segovia, *Rev. Esp. Quimioter.*, 2012, **25**, 1.
8. R. Viotti, B. Alarcon de Noya, T. Araujo-Jorge, M. J. Grijalva, F. Guhl, M. C. Lopez, J. M. Ramsey, I. Ribeiro, A. G. Schijman, S. Sosa-Estani, F. Torrico, J. Gascon and N. Latin American Network for Chagas Disease, *Antimicrob. Agents Chemother.*, 2014, **58**, 635.
9. A. V. Pinto and S. L. de Castro, *Molecules*, 2009, **14**, 4570.
10. C. O. Salas, M. Faundez, A. Morello, J. D. Maya and R. A. Tapia, *Curr. Med. Chem.*, 2011, **18**, 144.
11. M. L. Bolognesi, F. Lizzi, R. Perozzo, R. Brun and A. Cavalli, *Bioorg. Med. Chem. Lett.*, 2008, **18**, 2272.
12. R. A. Tapia, C. O. Salas, K. Vazquez, C. Espinosa-Bustos, J. Soto-Delgado, J. Varela, E. Birriel, H. Cerecetto, M. Gonzalez and M. Paulino, *Bioorg. Med. Chem. Lett.*, 2014, **24**, 3919.
13. I. Sieveking, P. Thomas, J. C. Estevez, N. Quinones, M. A. Cuellar, J. Villena, C. Espinosa-Bustos, A. Fierro, R. A. Tapia, J. D. Maya, R. Lopez-Munoz, B. K. Cassels, R. J. Estevez and C. O. Salas, *Bioorg. Med. Chem.*, 2014, **22**, 4609.
14. R. A. Tapia, L. Alegria, C. D. Pessoa, C. Salas, M. J. Cortes, J. A. Valderrama, M. E. Sarciron, F. Pautet, N. Walchshofer and H. Fillion, *Bioorg. Med. Chem.*, 2003, **11**, 2175.
15. C. Salas, R. A. Tapia, K. Ciudad, V. Armstrong, M. Orellana, U. Kemmerling, J. Ferreira, J. D. Maya and A. Morello, *Bioorg. Med. Chem.*, 2008, **16**, 668.
16. T. Aboul-Fadl, F. A. Bin-Jubair and O. Aboul-Wafa, *Eur. J. Med. Chem.*, 2010, **45**, 4578.
17. I. J. Chen and N. Foloppe, *J. Chem. Inf. Mod.*, 2008, **48**, 1773.
18. V. Prachayasittikul, R. Pingaew, A. Worachartcheewan, C. Nantasenamat, S. Prachayasittikul, S. Ruchirawat and V. Prachayasittikul, *Eur. J. Med. Chem.*, 2014, **84**, 247.
19. P. R. Duchowicz, D. O. Bennardi, D. E. Bacelo, E. L. Bonifazi, C. Rios-Luci, J. M. Padron, G. Burton and R. I. Misico, *Eur. J. Med. Chem.*, 2014, **77**, 176.
20. T. P. Jimenez Villalobos, R. Gaitan Ibarra and J. J. Montalvo Acosta, *J. Mol. Graph. Model.*, 2013, **46**, 105.
21. E. A. Hillard, F. C. de Abreu, D. C. Ferreira, G. Jaouen, M. O. Goulart and C. Amatore, *Chem. Commun.* 2008, 2612.
22. J. M. Miguel del Corral, M. A. Castro, M. Gordaliza, M. L. Martin, A. M. Gamito, C. Cuevas and A. S. Feliciano, *Bioorg. Med. Chem.*, 2006, **14**, 2816.
23. H. Hussain, K. Krohn, I. Ahmed, S. Draeger, B. Schulz, S. Pietro and G. Pescitelli, *Eur. J. Med. Chem.*, 2012, **9**, 1783.

RSC Advances Accepted Manuscript

24. T. A. D. Mendes, J. L. R. Cunha, R. D. Lourdes, G. F. R. Luiz, L. D. Lemos, A. R. R. dos Santos, A. C. J. da Camara, L. M. D. Galvao, C. Bern, R. H. Gilman, R. T. Fujiwara, R. T. Gazzinelli and D. C. Bartholomeu, *PloS Neglect. Trop. Dis.*, 2013, **7**, e2524.
25. E. Torres, E. Moreno-Viguri, S. Galiano, G. Devarapally, P. W. Crawford, A. Azqueta, L. Arbillaga, J. Varela, E. Birriel, R. Di Maio, H. Cerecetto, M. Gonzalez, I. Aldana, A. Monge and S. Perez-Silanes, *Eur. J. Med. Chem.*, 2013, **66**, 324.
26. G. Alvarez, J. Varela, P. Marquez, M. Gabay, C. E. Arias Rivas, K. Cuchilla, G. A. Echeverria, O. E. Piro, M. Chorilli, S. M. Leal, P. Escobar, E. Serna, S. Torres, G. Yaluff, N. I. Vera de Bilbao, M. Gonzalez and H. Cerecetto, *J. Med. Chem.*, 2014, **57**, 3999.
27. S. Nwaka and A. Hudson, *Nat. Rev. Drug Discov.*, 2006, **5**, 941.
28. A. J. Romanha, S. L. Castro, N. Soeiro Mde, J. Lannes-Vieira, I. Ribeiro, A. Talvani, B. Bourdin, B. Blum, B. Olivieri, C. Zani, C. Spadafora, E. Chiari, E. Chatelain, G. Chaves, J. E. Calzada, J. M. Bustamante, L. H. Freitas-Junior, L. I. Romero, M. T. Bahia, M. Lotrowska, M. Soares, S. G. Andrade, T. Armstrong, W. Degrave and A. Andrade Zde, *Mem. Inst. Oswaldo Cruz*, 2010, **105**, 233.
29. P. Kovacic, *Med. Hypotheses*, 2007, **69**, 510.
30. T. R. Henry and K. B. Wallace, *Arch. Toxicol.*, 1996, **70**, 482.
31. P. J. O'Brien, *Chem. Biol. Interac.*, 1991, **80**, 1.
32. J. Benites, J. A. Valderrama, K. Bettega, R. C. Pedrosa, P. B. Calderon and J. Verrax, *European J. Med. Chem.*, 2010, **45**, 6052.
33. J. M. Gutteridge and B. Halliwell, *Ann. NY Acad. Sci.*, 2000, **899**, 136.
34. J. F. Turrens, *Mol. Aspects Med.*, 2004, **25**, 211.
35. Z. Gonzalez-Chavez, V. Olin-Sandoval, J. S. Rodiguez-Zavala, R. Moreno-Sanchez and E. Saavedra, *Biochim. Biophys. Acta*, 2015, **1850**, 263.
36. V. Olin-Sandoval, R. Moreno-Sanchez and E. Saavedra, *Curr. Drug Targets*, 2010, **11**, 1614.
37. *Molecular Operating Environment (MOE)*, 2013.08; Chemical Computing Group Inc., 1010 Sherbooke St. West, Suite #910, Montreal, QC, Canada, H3A 2R7, 2013.
38. E. H. G. da Cruz, C. M. B. Hussene, G. G. Dias, E. B. T. Diogo, I. M. M. de Melo, B. L. Rodrigues, M. G. da Silva, W. O. Valenca, C. A. Camara, R. N. de Oliveira, Y. G. de Paiva, M. O. F. Goulart, B. C. Cavalcanti, C. Pessoa and E. N. da Silva, *Bioorg. Med. Chem.*, 2014, **22**, 1608.
39. E. B. T. Diogo, G. G. Dias, B. L. Rodrigues, T. T. Guimaraes, W. O. Valenca, C. A. Camara, R. N. de Oliveira, M. G. da Silva, V. F. Ferreira, Y. G. de Paiva, M. O. F. Goulart, R. F. S. Menna-Barreto, S. L. de Castro and E. N. da Silva, *Bioorg. Med. Chem.*, 2013, **21**, 6337.
40. F. M. Frank, A. B. Ciccarelli, M. Bollini, A. M. Bruno, A. Batlle and M. E. Lombardo, *Evid. Based Complement. Alternat. Med.,* 2013, **2013**, 10.
41. J. Rodriguez, A. Gerpe, G. Aguirre, U. Kemmerling, O. E. Piro, V. J. Aran, J. D. Maya, C. Olea-Azar, M. Gonzalez and H. Cerecetto, *Eur. J. Med. Chem.*, 2009, **44**, 1545.
42. F. C. de Abreu, P. A. D. Ferraz and M. O. F. Goulart, *J. Brazil Chem. Soc.*, 2002, **13**, 19.
43. G. Recabarren-Gajardo, M. Gacitua, I. Murueva, J. Romero, C. Espinosa-Bustos, J. Mella-Raipan, M. A. del Valle, C. D. Pessoa-Mahana and R. Tapia, *J. Phys. Org. Chem.*, 2011, **24**, 1179.
44. P. S. Guin, S. Das and P. C. Mandal, *Int. J. Electrochem. Sc.*, 2008, **3**, 1016.
45. E. N. da Silva, M. A. B. F. de Moura, A. V. Pinto, M. D. F. R. Pinto, M. C. B. V. de Souza, A. J. Araujo, C. Pessoa, L. V. Costa-Lotufo, R. C. Montenegro, M. O. de Moraes, V. F. Ferreira and M. O. F. Goulart, *J. Brazil Chem. Soc.*, 2009, **20**, 635.
46. E. Vicente, P. R. Duchowicz, D. Benitez, E. A. Castro, H. Cerecetto, M. Gonzalez and A. Monge, *Bioorg. Med. Chem. Lett.*, 2010, **20**, 4831.

RSC Advances Accepted Manuscript

47. M. A. Vera-Divaio, A. C. Freitas, H. C. Castro, S. de Albuquerque, L. M. Cabral, C. R. Rodrigues, M. G. Albuquerque, R. C. Martins, M. G. Henriques and L. R. Dias, *Bioorg. Med. Chem.*, 2009, **17**, 295.
48. G. Aguirre, M. Boiani, E. Cabrera, H. Cerecetto, R. Di Maio, M. Gonzalez, A. Denicola, C. M. Sant'anna and E. J. Barreiro, *Eur. J. Med. Chem.,* 2006, **41**, 457.
49. P. Tosco and T. Balle, *J. Mol. Model.*, 2011, **17**, 201.
50. P. Tosco, T. Balle and F. Shiri, *J. Comput. Aided Mol. Des.*, 2011, **25**, 777.
51. P. Tosco and T. Balle, *J. Chem. Inf. Model.,* 2012, **52**, 302.

RSC Advances Accepted Manuscript